

Spatially-resolved dynamics of the amplitude Schmid-Higgs mode in disordered superconductors

P. A. Nosov,¹ E. S. Andriyakhina,² and I. S. Burmistrov^{3,4}

¹*Department of Physics, Harvard University, Cambridge, Massachusetts 02138, USA*

²*Freie Universität Berlin, Dahlem Center for Complex Quantum Systems and Fachbereich Physik, Arnimallee 14, Berlin, 14195, Germany*

³*L.D. Landau Institute for Theoretical Physics, acad. Semenova av.1-a, Chernogolovka, 142432, Russia*

⁴*Laboratory for Condensed Matter Physics, HSE University, Moscow, 101000, Russia*

(Dated: March 11, 2025)

We investigate the spatially-resolved dynamics of the collective amplitude Schmid-Higgs (SH) mode in disordered s -wave superconductors and fermionic superfluids. By analyzing the analytic structure of the zero-temperature SH susceptibility in the complex frequency plane, we find that when the coherence length greatly exceeds the mean free path: (i) the SH response at fixed wave vectors exhibits late-time oscillations decaying as $1/t^2$ with frequency 2Δ , where Δ is the superconducting gap; (ii) sub-diffusive oscillations with a dynamical exponent $z=4$ emerge at late times and large distances; and (iii) spatial oscillations at fixed frequency decay exponentially, with a period that diverges as the frequency approaches 2Δ from above. When the coherence length is comparable to the mean free path, additional exponentially-decaying oscillations at fixed wave vectors appear with frequency above 2Δ . Furthermore, we show that the SH mode induces an extra peak in the third-harmonic generation current at finite wave-vectors. The frequency of this peak is shifted from the conventional resonance at Δ , thereby providing an unambiguous signature of order parameter amplitude dynamics.

Investigating the collective excitations in superconductors provides crucial insights into the complex structure of their order parameter and associated dynamical responses [1–6]. Unlike the well-studied phase fluctuations, the collective dynamics of the order parameter amplitude (so-called Schmid-Higgs (SH) mode) has received much less attention due to experimental challenges in its detection, primarily caused by its decoupling from density fluctuations. However, recent advances in terahertz and Raman spectroscopic probes have made direct observation of the SH mode more accessible [7–11], in turn prompting a renewed wave of theoretical interest in the amplitude fluctuations [12–30].

The properties of the SH mode in a disorder-free limit are relatively well established in both three-dimensional (3D) [17, 24, 31, 32] and two-dimensional (2D) [17, 18, 29] systems, across weak and strong coupling regimes. However, real materials inevitably contain impurities or other structural imperfections, making it imperative to understand how disorder influences the fluctuations of the superconducting order parameter. Despite extensive research of collective responses in dirty superconductors [26, 33–43], a comprehensive description of the spatially-resolved SH dynamics in this limit is still lacking. In particular, the dispersion relation and the associated long-distance and late-time oscillatory behavior of the SH mode in the presence of disorder remain unknown. Another open question is how the SH mode contributes to the nonlinear current response at finite wave vectors.

The goal of the present Letter is to fill this gap by examining the non-analyticities of the $T=0$ disorder-averaged SH susceptibility $\chi_{\text{SH}}(z, \mathbf{q})$ as a function of

complex frequency and momentum. This susceptibility quantifies the dynamical response of the order parameter amplitude $|\Delta(t, \mathbf{r})|$ that arises when external perturbations disturb it from its equilibrium state. Our approach is based on the BCS model with impurities, assuming a local attractive coupling λ that induces an s -wave, spin-singlet superconducting state with a zero-temperature gap Δ . For concreteness, we consider the following Hamiltonian density

$$\mathcal{H} = \sum_{\sigma} \psi_{\sigma}^{\dagger} \left(-\frac{(\nabla - i\mathbf{A})^2}{2m} - \mu + V(\mathbf{r}) \right) \psi_{\sigma} - \frac{\lambda}{\nu} \psi_{\uparrow}^{\dagger} \psi_{\downarrow}^{\dagger} \psi_{\downarrow} \psi_{\uparrow} \quad (1)$$

Here $\sigma=\uparrow/\downarrow$ labels spin degrees of freedom, ν is the density of states at the Fermi level in the normal state, $\lambda>0$ is the dimensionless BCS coupling constant, $\psi_{\sigma}(\mathbf{r})$ is the electron field, \mathbf{A} is the vector potential, and $V(\mathbf{r})$ is a white-noise Gaussian random potential that induces elastic scattering rate $1/\tau$. We assume that both $1/\tau$ and the superconducting gap Δ are much smaller than the Fermi energy, $\mu=mv_F^2/2$ (v_F is the Fermi velocity and m is the electron mass), which allows us to linearize the electron dispersion, and treat impurity scattering within the self-consistent Born approximation. The ratio $\Delta\tau$ is used to interpolate between the dirty ($\Delta\tau\ll 1$) and clean ($\Delta\tau\gg 1$) regimes. Under these conditions, the interplay of superconductivity and disorder is treated at the level of Anderson's theorem [44–46], disregarding more subtle effects such as interference-induced corrections [47–50], or spatial inhomogeneity of the order parameter and Lifshitz tails below the spectral edge [51–53].

SH susceptibility. The collective dynamics of the superconducting order parameter is described by the standard

Ginzburg-Landau functional obtained from Eq. (1) at $\mathbf{A}=0$, with its quadratic part encoding Gaussian fluctuations of the amplitude $|\Delta|$ around its mean-field value [54]

$$S_{\Delta\Delta} = \int_{\mathbf{r}} \sum_n \Delta(i\omega_n, \mathbf{r}) \chi_{\text{SH}}^{-1}(i\omega_n, \mathbf{r}, \mathbf{r}') \Delta(-i\omega_n, \mathbf{r}') \quad (2)$$

$$\chi_{\text{SH}}^{-1}(i\omega_n, \mathbf{r}, \mathbf{r}') = \lambda^{-1} \delta(\mathbf{r} - \mathbf{r}') - \Pi_{\Delta\Delta}(i\omega_n, \mathbf{r}, \mathbf{r}'),$$

where $\omega_n=2\pi Tn$ is the bosonic Matsubara frequency, χ_{SH} is the real space Matsubara SH susceptibility in a given disorder realization, and $\Pi_{\Delta\Delta}(i\omega_n, \mathbf{r}, \mathbf{r}')$ is the Fourier transform of the imaginary time correlation function $(\pi\nu)^{-1} \langle \mathcal{T} \hat{\Delta}(\tau, \mathbf{r}) \hat{\Delta}(0, \mathbf{r}') \rangle$. Here $\hat{\Delta}(\tau, \mathbf{r})$ is the s -wave, spin-singlet order parameter amplitude.

The expectation value is taken in the standard BCS state with the uniform mean-field order parameter Δ determined via the gap equation $1=\pi\lambda T \sum_m 1/E_{\varepsilon_m}$. Here $E_{\varepsilon_m}=\sqrt{\varepsilon_m^2+\Delta^2}$, and $\varepsilon_m=2\pi T(m+1/2)$ is the fermionic Matsubara frequency.

In this setup, the disorder-averaged Matsubara SH susceptibility $\chi_{\text{SH}}(i\omega_n, \mathbf{q})$ is given by [55]

$$\frac{1}{\chi_{\text{SH}}} = \pi T \sum_m \left\{ \frac{1}{E_{\varepsilon_m}} - S_{\mathbf{q}}(E_{\varepsilon_m} + E_{\tilde{\varepsilon}_m}) \left[1 + \frac{\varepsilon_m \tilde{\varepsilon}_m - \Delta^2}{E_{\varepsilon_m} E_{\tilde{\varepsilon}_m}} \right] \right\}, \quad (3)$$

where $\tilde{\varepsilon}_m = \varepsilon_m + |\omega_n|$. This expression assumes $q \ll mv_F$, but fully captures the crossover between the diffusive and ballistic scales through the structure factor $S_{\mathbf{q}}(E)$. It is given by $S_{\mathbf{q}}^{2\text{D}}(E) = 1/(|\mathcal{E}| - 1/\tau)$ for a 2D system and by $S_{\mathbf{q}}^{3\text{D}}(E) = 1/(v_F q / \arg \mathcal{E} - 1/\tau)$ in 3D, where $\mathcal{E} = E + 1/\tau + i v_F q$. In the diffusive limit, $v_F q, E \ll 1/\tau$, the structure factor in Eq. (3) reduces to [4, 33, 56]

$$S_{\mathbf{q}}(E) = 1/(Dq^2 + E), \quad D = v_F^2 \tau / d, \quad (4)$$

where $d=2, 3$ is the dimensionality. At $q=0$, Eq. (3) reduces to its clean limit for any $\Delta\tau$ as a manifestation of Anderson's theorem.

The retarded SH susceptibility $\chi_{\text{SH}}^R(\omega, \mathbf{q})$ at $T=0$ is obtained from Eq. (3) in a standard way [55]. The branch cuts are chosen along the real axis such that for any real $|E| \geq \Delta$ we have $\sqrt{\Delta^2 - (E \pm i0)^2} = \mp i \text{sgn}(E) \sqrt{E^2 - \Delta^2}$. If extended to the lower half-plane as well, the above choice of the branch cut defines the *physical* Riemann sheet of $\chi_{\text{SH}}(z, \mathbf{q})$, with its imaginary part changing discontinuously across the cut along the real axis at $|\text{Re } z| \geq 2\Delta$, and vanishing for $\text{Im } z=0, |\text{Re } z| \leq 2\Delta$ due to the presence of the superconducting gap (see Fig. 1). The resulting Cauchy representation of $[\chi_{\text{SH}}(z, \mathbf{q})]^{-1}$ on the physical sheet is given by

$$\frac{1}{\chi_{\text{SH}}} = \int_{-\infty}^{+\infty} \frac{d\varepsilon}{\pi} \left[\frac{\rho_{\mathbf{q}}(|\varepsilon|) \text{sgn } \varepsilon}{\varepsilon - z} + \frac{\pi/2}{\sqrt{\varepsilon^2 - 4\Delta^2}} \right] \theta\left(\frac{|\varepsilon|}{2\Delta} - 1\right) \quad (5)$$

for $z \in \mathbb{C} / \{z: \text{Im } z=0, |\text{Re } z| \geq 2\Delta\}$. The second term in Eq. (5) arises because $1/|\chi_{\text{SH}}(\omega_n, \mathbf{q})|$ is an increasing

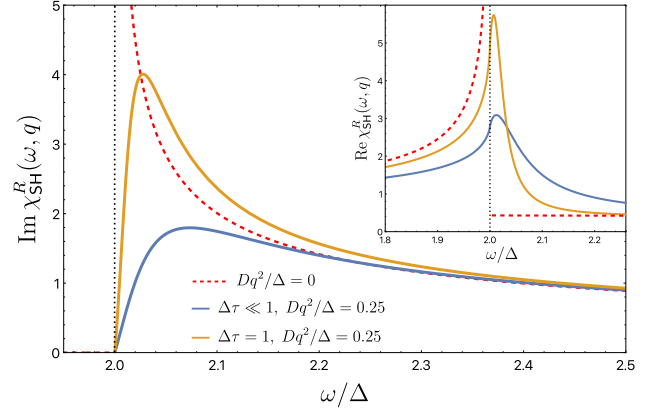


FIG. 1. The spectral function $\text{Im } \chi_{\text{SH}}^R(\omega, \mathbf{q})$ for $Dq^2/\Delta=0.25$ ($\xi q=0.5$). The blue (orange) curve corresponds to $\Delta\tau \ll 1$ ($\Delta\tau=1$) in 2D. The dotted line indicates the continuum edge. The dashed red line corresponds to $q=0$ independent of $\Delta\tau$. Inset: $\text{Re } \chi_{\text{SH}}^R(\omega, \mathbf{q})$ for the same parameters.

function of ω_n , see [55] for details. This relation allows us to immediately interpret the spectral density $\text{sgn}(\varepsilon)\theta(|\varepsilon|-2\Delta)\rho_{\mathbf{q}}(|\varepsilon|)$ in Eq. (5) as $\text{Im}[1/\chi_{\text{SH}}^R(\varepsilon, \mathbf{q})]$, whereas the real part is obtained by taking the principal value of the integral. The full expression for $\rho_{\mathbf{q}}(\omega)$ is given in [55], and its diffusive limit at $\Delta\tau \ll 1$ yields

$$\rho_{\mathbf{q}}(\omega) = \frac{4\bar{\omega}^2 - (\bar{q}^4 + \bar{\omega}^2)^2}{\bar{q}^2(\bar{\omega}+2)(\bar{q}^4 + \bar{\omega}^2)} \Pi\left(\frac{(\bar{\omega}-2)^2(\bar{q}^4 + \bar{\omega}^2)}{\bar{q}^4(4 - \bar{q}^4 - \bar{\omega}^2)} \middle| \frac{\bar{\omega}-2}{\bar{\omega}+2}\right) + \frac{\bar{q}^2(4 + \bar{q}^4 + \bar{\omega}^2)}{(\bar{\omega}+2)(\bar{q}^4 + \bar{\omega}^2)} K\left(\frac{\bar{\omega}-2}{\bar{\omega}+2}\right). \quad (6)$$

Here, we defined dimensionless variables $\bar{\omega}=\omega/\Delta$, $\bar{q}=\xi q$, and $\xi=\sqrt{D/\Delta}$ is the coherence length. Also, $\Pi(x|y) = \int_0^{\pi/2} d\alpha / ((1-x \sin^2 \alpha) \sqrt{1-y^2 \sin^2 \alpha})$ is the complete elliptic integral of the 3rd kind, and $K(x) = \Pi(0|x)$. Eq. (6) only assumes $|\omega|, v_F q \ll 1/\tau$, but ξq and $|\omega|/\Delta$ can be arbitrary.

The imaginary and real parts of $\chi_{\text{SH}}^R(\omega, \mathbf{q})$ at $q>0$ feature a peak at a frequency above 2Δ for arbitrary values of $\Delta\tau$, as shown in Fig. 1. This peak shifts to higher frequencies when momentum is increased. At $q=0$, the peak is replaced with a square-root singularity at $\omega=2\Delta$ [1]. Further assuming the dirty limit, $\xi q \ll 1$ and $0 \leq \omega - 2\Delta \ll \Delta$, while keeping the ratio $\Delta \xi^4 q^4 / (\omega - 2\Delta)$ fixed (i.e. anticipating the $z=4$ dynamical exponent, defined by the relation $|\omega - 2\Delta| \sim q^z$), we obtain

$$\frac{1}{\chi_{\text{SH}}^R} \simeq \frac{\bar{q}^2}{4} \left[\ln \frac{2^6}{\bar{q}^4} - \sum_{s=\pm} (1+su) \ln(u+s) + i\pi(1-u) \right], \quad (7)$$

where $u = \sqrt{1+4(\bar{\omega}-2)/\bar{q}^4} \geq 1$. From Eq. (7), we find that the frequency and the width of the peak in χ_{SH}^R at $\xi q \ll 1$

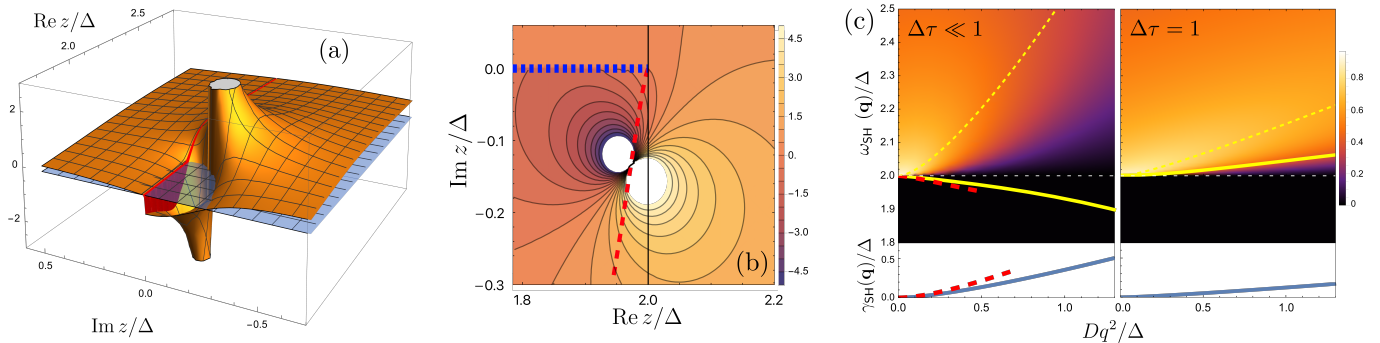


FIG. 2. (a) $\text{Im} \chi_{\text{SH}}^{\downarrow}(z, \mathbf{q})$ (orange surface) in the complex frequency plane for $Dq^2/\Delta=0.5$ and $\Delta\tau \ll 1$. The red solid line corresponds to the real axis $\text{Im} z=0$, and the red vertical region indicates the discontinuity in $\text{Im} \chi_{\text{SH}}^{\downarrow}(z, \mathbf{q})$ along its branch cut. The transparent blue plane marks zero on the vertical axis. (b) The contour plot of $\text{Im} \chi_{\text{SH}}^{\downarrow}(z, \mathbf{q})$ for the same parameters. The blue dashed line indicated the branch cut of $\chi_{\text{SH}}^{\downarrow}(z, \mathbf{q})$. The red dashed line shows the trajectory of the pole while momentum is varied. (c) The frequency of the SH mode as a function of $\xi^2 q^2 \equiv Dq^2/\Delta$ for $\Delta\tau \ll 1$ (left panel) and $\Delta\tau=1$ (right panel) in 2D, shown with a yellow solid curve. The small- q asymptotic behavior, Eq. (B2), is shown with the dashed red curve. The normalized spectral function $2 \arctan(\text{Im} \chi_{\text{SH}}^R(\omega, \mathbf{q}))/\pi \in [0, 1]$ is shown with the background color. The yellow dashed line shows the position of the maximum of the spectral function. The horizontal white dashed line denotes the edge of the two-particle continuum. The SH damping rate (blue solid curve) is shown at the bottom.

[55] scale as

$$\frac{\omega_{\text{max}}(\mathbf{q})}{\Delta} \approx 2 + \frac{4\xi^4 q^4}{\pi^2} \ln^2 \frac{2\sqrt{2}}{\xi q}, \quad \frac{\gamma_{\text{max}}(\mathbf{q})}{\Delta} \sim \xi^4 q^4 \ln \frac{1}{\xi q}. \quad (8)$$

To calculate the late-time and long-distance behavior of the SH susceptibility, we now proceed to identify its non-analyticities (e.g., poles) in the complex plane.

SH mode as a pole in the SH susceptibility. The appearance of a peak in $\chi_{\text{SH}}^R(\omega, \mathbf{q})$ on the real frequency axis is already indicative of a pole in the lower half-plane. However, as emphasized above, the presence of the branch cut implies that $\chi_{\text{SH}}(\omega+i0^+, \mathbf{q})$ is not smoothly connected to $\chi_{\text{SH}}(\omega-i0^+, \mathbf{q})$. In fact, $\chi_{\text{SH}}(z, \mathbf{q})$ does not have any non-analyticities in the lower half-plane on the physical Riemann sheet. Instead, one has to smoothly continue it through the branch cut into the *unphysical* Riemann sheet, and search for a pole there [24, 29, 31]. The resulting susceptibility, denoted as $\chi_{\text{SH}}^{\downarrow}(z, \mathbf{q})$, coincides with Eq. (5) in the upper half-plane, but remains continuous across the interval $\text{Im} z=0$, $\text{Re} z > 2\Delta$. The structure of $\chi_{\text{SH}}^{\downarrow}(z, \mathbf{q})$ is demonstrated in Fig. 2(a,b), and the explicit formula for it is given in End Matter. Numerical evaluation reveals that $\chi_{\text{SH}}^{\downarrow}(z, \mathbf{q})$ indeed has a pole $z_{\mathbf{q}}$ in the lower half-plane at any finite momentum q . The SH mode's dispersion is then obtained as $\omega_{\text{SH}}(\mathbf{q}) \equiv \text{Re} z_{\mathbf{q}}$ and $\gamma_{\text{SH}}(\mathbf{q}) \equiv |\text{Im} z_{\mathbf{q}}|$, with both of these quantities exhibiting strong dependence on $\Delta\tau$ (see Fig. 2(c)). In the dirty limit $\Delta\tau \ll 1$, for $\xi q \ll 1$ we obtain

$$\frac{\omega_{\text{SH}}(\mathbf{q})}{\Delta} \approx 2 - \frac{4\xi^4 q^4}{\pi^2} \ln^2 \frac{2\sqrt{\pi}}{\xi q}, \quad \frac{\gamma_{\text{SH}}(\mathbf{q})}{\Delta} \approx \frac{4\xi^4 q^4}{\pi} \ln \frac{2\sqrt{\pi}}{\xi q} \quad (9)$$

The $z=4$ scaling of $\omega_{\text{SH}}(\mathbf{q})$ with momentum can be also

estimated directly from $S_{\mathbf{q}}(E)$ in Eq. (4) since the SH mode involves quasiparticles with energy $\omega \gtrsim \Delta$. Expanding $S_{\mathbf{q}}(\sqrt{\omega^2 - \Delta^2})$ for such ω , we find that the pole occurs at $|\omega - \Delta| \sim D^2 q^4 / \Delta$ in the dirty limit. We also emphasize that $\omega_{\text{SH}}(\mathbf{q}) < 2\Delta$. In the terminology of Ref. [57], the pole is “hidden” behind the branch cut of $\chi_{\text{SH}}^{\downarrow}(z, \mathbf{q})$ on the real axis at $\text{Re} z < 2\Delta$ (see Fig. 2(b,c)). Upon increasing $\Delta\tau$ while keeping ξq fixed, the pole $z_{\mathbf{q}}$ shifts to the right. Eventually, its frequency $\omega_{\text{SH}}(\mathbf{q})$ exceeds 2Δ — that is, the pole becomes “visible” — and it contributes to the Fourier transform, giving rise to additional exponentially decaying oscillations at frequency $\omega_{\text{SH}}(\mathbf{q})$ in $\chi_{\text{SH}}^R(t, \mathbf{q})$ (cf. Eq. (10)). At moderate values of $\Delta\tau \approx 1$, the dispersion develops a quadratic dependence on q (see Fig. 2(c)). The results of Refs. [29, 31] are recovered in the limit $\Delta\tau \rightarrow \infty$ (see [55] for a detailed analysis of the crossover between the dirty and clean regimes). A similar analysis of the SH susceptibility in the complex momentum plane at fixed $\bar{\omega}$ also reveals a pole [55].

Late-time and long-distance SH oscillations. Let us now discuss how the aforementioned pole manifests itself in various asymptotic limits of χ_{SH}^R . First, we consider $\chi_{\text{SH}}^R(t, \mathbf{q})$ at late times t and fixed momentum, which describes a response to a sudden, spatially periodic perturbation. For arbitrary $\Delta\tau$, we find

$$\chi_{\text{SH}}^R(t, \mathbf{q}) \simeq 2 \text{Im}[Z_{\mathbf{q}} e^{-i\omega_{\text{SH}}(\mathbf{q})t}] e^{-\gamma_{\text{SH}}(\mathbf{q})t} \theta(\omega_{\text{SH}}(\mathbf{q}) - 2\Delta) - \frac{2 \sin(2\Delta t)}{\pi t^2} \partial_{\omega} \text{Im} \chi_{\text{SH}}^R(\omega, \mathbf{q})_{\omega=2\Delta+0^+}, \quad (10)$$

where $Z_{\mathbf{q}}$ is the residue of $\chi_{\text{SH}}^{\downarrow}(z, \mathbf{q})$ at $z_{\mathbf{q}}$. The asymptotic late-time behavior is determined by the second term stemming from the continuum edge at $\omega=2\Delta$ in $\text{Im} \chi_{\text{SH}}^R$. These oscillations at frequency 2Δ decay as $1/t^2$, in

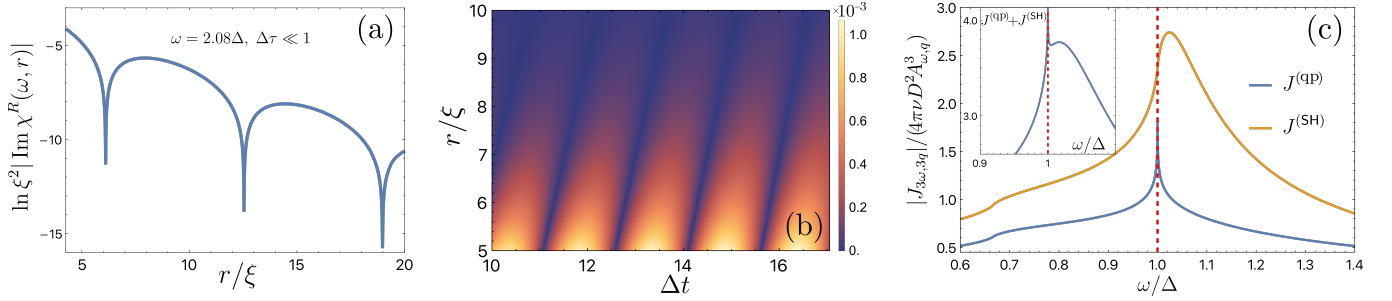


FIG. 3. Oscillations in (a) $\ln \xi^2 |\text{Im} \chi_{\text{SH}}^R(\omega, r)|$ and in (b) $|\xi^2 \chi_{\text{SH}}^R(t, r)/\Delta|$ in 2D, and in the dirty limit $\Delta\tau \ll 1$. (c) The absolute value of the individual contributions to the current for $Dq^2/\Delta=1/8$ for $\Delta\tau \ll 1$. The red dashed line indicates the $q=0$ resonance at $\omega=\Delta$. The blue (orange) curve corresponds to the quasiparticle (Schmid-Higgs) contribution. The inset shows the total current.

contrast to the conventional $\sim 1/\sqrt{t}$ decay at $q=0$ [1]. The first term in Eq. (10) originates from the pole z_q , provided that its real part, $\omega_{\text{SH}}(\mathbf{q})$, exceeds 2Δ . Although this exponentially decaying contribution is sub-leading, interestingly, its frequency is q -dependent. In the dirty limit, the pole is “hidden” by the branch cut ($\omega_{\text{SH}}(\mathbf{q}) < 2\Delta$, see Fig. 2(a,b)) so its contribution to χ_{SH}^R is strongly incoherent and does not produce oscillations. Thus for $\Delta\tau \ll 1$ and $\xi q \ll 1$, Eq. (10) yields

$$\chi_{\text{SH}}^R(t, \mathbf{q}) \approx -\sin(2\Delta t)/[\Delta t^2 (\xi q)^6 \ln^2(\xi q/2)]. \quad (11)$$

At moderate disorder (or large momentum), the SH pole shifts into the right half-plane ($\omega_{\text{SH}} > 2\Delta$) and becomes “visible” (cf. Fig. 2(c)), resulting in a coherent feature in χ_{SH}^R and additional oscillations (first term in Eq. (10)). The “critical” q_c at which these oscillations first appear (i.e. $\omega_{\text{SH}}(q_c) = 2\Delta$) is analyzed in [55].

The long-distance oscillations of $\chi_{\text{SH}}^R(\omega, \mathbf{r})$ at a fixed frequency ω are closely related to the pole in χ_{SH}^R in the complex momentum space. These oscillations correspond to a spatially-local periodic external drive and exist for $\omega > 2\Delta$ only. In 2D and in the dirty limit, $\Delta\tau \ll 1$, we find

$$\text{Im} \chi_{\text{SH}}^R(\omega, \mathbf{r}) \simeq \frac{2^{1/4} \sqrt{\xi_\omega/r}}{\sqrt{\pi} \xi^2 \ln \frac{2^4 \Delta}{\omega - 2\Delta}} e^{-r/\xi_\omega} \sin\left(\frac{r}{\xi_\omega} + \frac{\pi}{8}\right), \quad (12)$$

where $\xi_\omega = \xi [|\ln((\frac{\omega}{\Delta} - 2)/2^4)|^2 / (\pi^2 (\frac{\omega}{\Delta} - 2))]^{1/4}$ is the period of oscillations diverging at the threshold $\omega = 2\Delta$.

The long-distance and late-time behavior of $\chi_{\text{SH}}^R(t, \mathbf{r})$ in the regime $\Delta\tau \ll 1$ is sub-diffusive, featuring oscillations as a function of $\varkappa = \pi^2 (r/\xi)^4 / (\Delta t) \ln^2(\Delta t)$ with an approximate dynamical exponent $z=4$ (which implies the relation $r \sim t^{1/z}$). In 2D, for $\varkappa \gg 1$, we find

$$\chi_{\text{SH}}^R(t, \mathbf{r}) \simeq \frac{2^{3/4} e^{-\frac{3\sqrt{3}}{8} \varkappa^{1/3}}}{\sqrt{3} \pi \xi^2 t \ln(\Delta t)} \cos\left(\frac{3}{8} \varkappa^{1/3} - 2\Delta t\right). \quad (13)$$

In the opposite regime, $\Delta\tau \gg 1$, the amplitude SH fluctuations propagate diffusively, with $z=2$. Oscillations (13) can be induced by a quenched perturbation affecting a

local gap magnitude. The results in 3D are qualitatively similar to Eqs. (12)-(13) and are presented in [55]. The analytic results (12)-(13) are benchmarked against direct numerical evaluation of χ_{SH}^R shown in Fig. 3.

SH mode and the nonlinear current response. The results for χ_{SH} outlined above can be directly probed via the electromagnetic response to an external harmonic vector potential $\mathbf{A}(t, \mathbf{r}) = \mathbf{A}_{\omega, \mathbf{q}} e^{i\mathbf{q}\cdot\mathbf{r} - i\omega t}$. As well-known, at cubic order in $\mathbf{A}_{\omega, \mathbf{q}}$, induced corrections to the amplitude fluctuations at frequency 2ω and momentum $2\mathbf{q}$ lead to the current oscillations at frequency 3ω and momentum $3\mathbf{q}$ – the effect known as third harmonic generation (THG) [8, 19, 20, 25, 26]. After evaluating the diagrams familiar from the $q=0$ case [26], we find that the resulting paramagnetic contribution to the current (which is absent in the clean case [6, 20]) consists of two terms, $\mathbf{J}_{3\omega, 3\mathbf{q}} = \mathbf{J}_{3\omega, 3\mathbf{q}}^{(\text{qp})} + \mathbf{J}_{3\omega, 3\mathbf{q}}^{(\text{SH})}$ (see End Matter). The first term corresponds to a direct quasiparticle (qp) channel, and the second one involves the SH susceptibility:

$$\mathbf{J}_{3\omega, 3\mathbf{q}}^{(\text{SH})} = 4\pi\nu D^2 \chi_{\text{SH}}^R(2\omega, 2\mathbf{q}) \mathcal{B}_{\text{SH}}^R(\omega, \mathbf{q}) |\mathbf{A}_{\omega, \mathbf{q}}|^2 \mathbf{A}_{\omega, \mathbf{q}}. \quad (14)$$

The lengthy expression for $\mathcal{B}_{\text{SH}}^R(\omega, \mathbf{q})$ is given in [55]. Unlike the SH susceptibility $\chi_{\text{SH}}^R(2\omega, 2\mathbf{q})$, $\mathcal{B}_{\text{SH}}^R(\omega, \mathbf{q})$ does not exhibit any sharp non-analytic features in the limit $q \rightarrow 0$ and $\omega \rightarrow \Delta$ and it could be replaced in Eq. (14) with its limiting value $\mathcal{B}_{\text{SH}}^R(\Delta, 0) \approx -1.55 - 1.27i$. Consequently, for $|\omega - \Delta| \ll \Delta$, the current $\mathbf{J}_{3\omega, 3\mathbf{q}}^{(\text{SH})}$ is essentially governed by the SH susceptibility and exhibits a peak at a frequency $\omega_{\text{max}}(\mathbf{q})/2 > \Delta$ with the height that scales as $1/(\xi q)^2$, see Eq. (8) and Fig. 3(c). In contrast, we find that the peak in the “quasiparticle” contribution $\mathbf{J}_{3\omega, 3\mathbf{q}}^{(\text{qp})}$ remains fixed at Δ even for $q \neq 0$, as shown in Fig. 2(c). Intuitively, this is expected because the momentum-resolved collective dynamics of the order parameter fluctuations is very distinct from individual quasiparticle excitations. Since $\mathbf{J}_{3\omega, 3\mathbf{q}}^{(\text{qp})}$ at $\omega = \omega_{\text{max}}(\mathbf{q})/2$ grows as $\ln[1/(\xi q)]$ only (see End Matter), the peak in SH contribution dominates the quasiparticle contribution at $\xi q \ll 1$. The pair-breaking effects (e.g. magnetic impurities) will broaden both peaks, thereby establishing

a lower bound on q for observation of the SH peak in the THG. Thus, the emergence of an additional peak at a frequency above Δ in the finite-momentum current provides an unambiguous signature of the amplitude SH fluctuations and allows for a direct investigation of their dynamics summarized by Eqs. (11)-(13).

Conclusions. In this work, we studied the spatially-resolved dynamics of the order parameter amplitude (SH) fluctuations in BCS superconductors with non-magnetic impurities. We identified a pole on the unphysical Riemann sheet of the SH susceptibility, associated with the oscillatory mode exhibiting sub-diffusive $z=4$ spreading in the dirty limit. This pole also produces a peak in the spectral function above the edge of the two-particle continuum, even though the frequency of the SH mode itself can be below 2Δ for sufficiently strong disorder. We also calculated the contribution of the SH mode to the non-linear current response, focusing on the THG. We found that at finite wave vectors, the THG current exhibits an additional peak in its amplitude, shifted away from the conventional resonance at $\omega=\Delta$. This extra peak arises solely from the dynamics of the amplitude SH mode. Importantly, both disorder and finite wave vectors are essential for this effect. Without disorder, the SH mode would not contribute to the current [20], and at zero wave vector, multiple processes conflate into a single peak at Δ [26], making it difficult to disentangle the SH contribution. Our findings could be directly tested with spatially-resolved terahertz and Raman spectroscopic probes [7–10]. Moreover, a finite wave vector can be imprinted in the current response in thin films with high-frequency surface acoustic waves [58, 59], diffraction gratings and micropatterning [60], finite spot size of the pump pulse [6, 61], or by adding extra layers of a 2D van der Waals material with a Moiré superlattice. Another promising possibility is to use spatially-inhomogeneous Feshbach modulation of the interaction strength in disordered cold gases [62] to directly quench the local value of the gap and study its spatial relaxation [63].

Acknowledgments. – We thank A. Chubukov, A. Mel’nikov, V. Kravtsov, S. Raghu, and A. Levchenko for fruitful discussions. The work of P.A.N. was supported in part by the US Department of Energy, Office of Basic Energy Sciences, Division of Materials Sciences and Engineering, under contract number DE-AC02-76SF00515. The work of I.S.B. was supported by the Russian Ministry of Science and Higher Education and by the Basic Research Program of HSE. I.S.B. acknowledges personal support from the Foundation for the Advancement of Theoretical Physics and Mathematics “BASIS”.

[1] V. Vaks, V. Galitskii, and A. Larkin, Collective excitations in a superconductor, *Sov. Phys. JETP* **14**, 1177

- (1962).
- [2] A. Schmid, The approach to equilibrium in a pure superconductor: The relaxation of the Cooper pair density, *Phys. Status Solidi (b)* **8**, 129 (1968).
- [3] S. N. Artemenko and A. F. Volkov, Electric fields and collective oscillations in superconductors, *Sov. Phys. Usp.* **22**, 295 (1979).
- [4] I. O. Kulik, O. Entin-Wohlman, and R. Orbach, Pair susceptibility and mode propagation in superconductors: A microscopic approach, *J. Low Temp. Phys.* **43**, 591 (1981).
- [5] P. I. Arseev, S. O. Loiko, and N. K. Fedorov, Theory of gauge-invariant response of superconductors to an external electromagnetic field, *Phys. Usp.* **49**, 1 (2006).
- [6] R. Shimano and N. Tsuji, Higgs mode in superconductors, *Annu. Rev. Condens. Matter Phys.* **11**, 103 (2020).
- [7] R. Matsunaga, Y. I. Hamada, K. Makise, Y. Uzawa, H. Terai, Z. Wang, and R. Shimano, Higgs amplitude mode in the BCS superconductors $\text{Nb}_{1-x}\text{Ti}_x\text{N}$ induced by terahertz pulse excitation, *Phys. Rev. Lett.* **111**, 057002 (2013).
- [8] R. Matsunaga, N. Tsuji, H. Fujita, A. Sugioka, K. Makise, Y. Uzawa, H. Terai, Z. Wang, H. Aoki, and R. Shimano, Light-induced collective pseudospin precession resonating with Higgs mode in a superconductor, *Science* **345**, 1145 (2014).
- [9] D. Sherman, U. S. Pracht, B. Gorshunov, S. Poran, J. Jesudasan, M. Chand, P. Raychaudhuri, M. Swanson, N. Trivedi, A. Auerbach, *et al.*, The Higgs mode in disordered superconductors close to a quantum phase transition, *Nat. Phys.* **11**, 188 (2015).
- [10] R. Grasset, T. Cea, Y. Gallais, M. Cazayous, A. Sacuto, L. Cario, L. Benfatto, and M.-A. Méasson, Higgs-mode radiance and charge-density-wave order in 2H-NbSe_2 , *Phys. Rev. B* **97**, 094502 (2018).
- [11] K. Katsumi, J. Fiore, M. Udina, R. Romero, D. Barbalas, J. Jesudasan, P. Raychaudhuri, G. Seibold, L. Benfatto, and N. P. Armitage, Revealing novel aspects of light-matter coupling by terahertz two-dimensional coherent spectroscopy: The case of the amplitude mode in superconductors, *Phys. Rev. Lett.* **132**, 256903 (2024).
- [12] i. c. v. Kos, A. J. Millis, and A. I. Larkin, Gaussian fluctuation corrections to the BCS mean-field gap amplitude at zero temperature, *Phys. Rev. B* **70**, 214531 (2004).
- [13] R. Combescot, M. Y. Kagan, and S. Stringari, Collective mode of homogeneous superfluid Fermi gases in the BEC-BCS crossover, *Phys. Rev. A* **74**, 042717 (2006).
- [14] R. A. Barankov and L. S. Levitov, Synchronization in the bcs pairing dynamics as a critical phenomenon, *Phys. Rev. Lett.* **96**, 230403 (2006).
- [15] E. A. Yuzbashyan, O. Tsyplatyev, and B. L. Altshuler, Relaxation and persistent oscillations of the order parameter in fermionic condensates, *Phys. Rev. Lett.* **96**, 097005 (2006).
- [16] M. Dzero, E. A. Yuzbashyan, and B. L. Altshuler, Cooper pair turbulence in atomic Fermi gases, *Europhys. Lett.* **85**, 20004 (2009).
- [17] D. Podolsky, A. Auerbach, and D. P. Arovas, Visibility of the amplitude (higgs) mode in condensed matter, *Phys. Rev. B* **84**, 174522 (2011).
- [18] S. Gazit, D. Podolsky, and A. Auerbach, Fate of the higgs mode near quantum criticality, *Phys. Rev. Lett.* **110**, 140401 (2013).
- [19] N. Tsuji and H. Aoki, Theory of anderson pseudospin res-

- onance with higgs mode in superconductors, *Phys. Rev. B* **92**, 064508 (2015).
- [20] T. Cea, C. Castellani, and L. Benfatto, Nonlinear optical effects and third-harmonic generation in superconductors: Cooper pairs versus higgs mode contribution, *Phys. Rev. B* **93**, 180507 (2016).
- [21] A. Moor, A. F. Volkov, and K. B. Efetov, Amplitude Higgs mode and admittance in superconductors with a moving condensate, *Phys. Rev. Lett.* **118**, 047001 (2017).
- [22] S. Fischer, M. Hecker, M. Hoyer, and J. Schmalian, Short-distance breakdown of the Higgs mechanism and the robustness of the BCS theory for charged superconductors, *Phys. Rev. B* **97**, 054510 (2018).
- [23] P. Shen and M. Dzero, Gaussian fluctuation corrections to a mean-field theory of complex hidden order in URu₂Si₂, *Phys. Rev. B* **98**, 125131 (2018).
- [24] H. Kurkjian, S. N. Klimin, J. Tempere, and Y. Castin, Pair-breaking collective branch in BCS superconductors and superfluid Fermi gases, *Phys. Rev. Lett.* **122**, 093403 (2019).
- [25] Y. Murotani and R. Shimano, Nonlinear optical response of collective modes in multiband superconductors assisted by nonmagnetic impurities, *Phys. Rev. B* **99**, 224510 (2019).
- [26] M. Silaev, Nonlinear electromagnetic response and higgs-mode excitation in bcs superconductors with impurities, *Phys. Rev. B* **99**, 224511 (2019).
- [27] Z. Sun, M. M. Fogler, D. N. Basov, and A. J. Millis, Collective modes and terahertz near-field response of superconductors, *Phys. Rev. Res.* **2**, 023413 (2020).
- [28] P. A. Lee and J. F. Steiner, Detection of collective modes in unconventional superconductors using tunneling spectroscopy, *Phys. Rev. B* **108**, 174503 (2023).
- [29] D. Phan and A. V. Chubukov, Following the Higgs mode across the BCS-BEC crossover in two dimensions, *Phys. Rev. B* **107**, 134519 (2023).
- [30] Y. Du, G. Liu, W. Ruan, Z. Fang, K. Watanabe, T. Taniguchi, R. Liu, J.-X. Li, and X. Xi, Unveiling resilient superconducting fluctuations in atomically thin nbse₂ through higgs mode spectroscopy, *Phys. Rev. Lett.* **134**, 066002 (2025).
- [31] V. A. Andrianov and V. N. Popov, Hydrodynamic action and Bose spectrum of superfluid Fermi systems, *Theoretical and Mathematical Physics* **28**, 829 (1976).
- [32] R. V. Carlson and A. M. Goldman, Superconducting order-parameter fluctuations below T_c , *Phys. Rev. Lett.* **31**, 880 (1973).
- [33] R. A. Smith, M. Y. Reizer, and J. W. Wilkins, Suppression of the order parameter in homogeneous disordered superconductors, *Phys. Rev. B* **51**, 6470 (1995).
- [34] M. Reizer, Electron-electron relaxation in two-dimensional impure superconductors, *Phys. Rev. B* **61**, 7108 (2000).
- [35] M. Mondal, A. Kamlapure, M. Chand, G. Saraswat, S. Kumar, J. Jesudasan, L. Benfatto, V. Tripathi, and P. Raychaudhuri, Phase fluctuations in a strongly disordered s-wave NbN superconductor close to the metal-insulator transition, *Phys. Rev. Lett.* **106**, 047001 (2011).
- [36] T. Cea, D. Bucheli, G. Seibold, L. Benfatto, J. Lorenzana, and C. Castellani, Optical excitation of phase modes in strongly disordered superconductors, *Phys. Rev. B* **89**, 174506 (2014).
- [37] T. Cea, C. Castellani, G. Seibold, and L. Benfatto, Non-relativistic dynamics of the amplitude (Higgs) mode in superconductors, *Phys. Rev. Lett.* **115**, 157002 (2015).
- [38] A. V. Shtyk and M. V. Feigel'man, Collective modes and ultrasonic attenuation in a pseudogapped superconductor, *Phys. Rev. B* **96**, 064523 (2017).
- [39] A. Kamenev, *Field theory of non-equilibrium systems* (Cambridge University Press, 2023).
- [40] Y. Li and M. Dzero, Amplitude Higgs mode in superconductors with magnetic impurities, *Phys. Rev. B* **109**, 054520 (2024).
- [41] Y. Li and M. Dzero, Collective modes in terahertz field response of superconductors with paramagnetic impurities, arXiv preprint arXiv:2403.03980 (2024).
- [42] B. Fan and A. M. G. García, Quenched dynamics and pattern formation in clean and disordered Bogoliubov-de Gennes superconductors, *SciPost Phys.* **17**, 049 (2024).
- [43] K. Wang, R. Boyack, and K. Levin, The higgs-amplitude mode in the optical conductivity in the presence of a supercurrent: Gauge invariant formulation, arXiv preprint arXiv:2411.18781 (2024).
- [44] P. W. Anderson, Theory of dirty superconductors, *J. Phys. Chem. Solid* **11**, 26 (1959).
- [45] A. A. Abrikosov and L. P. Gor'kov, On the theory of superconducting alloys, I. The electrodynamics of alloys at absolute zero, *Sov. Phys. JETP* **8**, 1090 (1959).
- [46] A. A. Abrikosov and L. P. Gor'kov, Superconducting alloys at finite temperatures, *Sov. Phys. JETP* **9**, 220 (1959).
- [47] S. Maekawa and H. Fukuyama, Localization effects in two-dimensional superconductors, *J. Phys. Soc. Jpn.* **51**, 1380 (1982).
- [48] S. Maekawa, H. Ebisawa, , and H. Fukuyama, Theory of dirty superconductors in weakly localized regime, *J. Phys. Soc. Jpn.* **53**, 2681 (1984).
- [49] A. M. Finkel'stein, Superconducting transition temperature in amorphous films, *JETP Lett.* **45**, 46 (1987).
- [50] A. M. Finkel'stein, Suppression of superconductivity in homogeneously disordered systems, *Physica B* **197**, 636 (1994).
- [51] A. Larkin and Y. N. Ovchinnikov, Density of states in inhomogeneous superconductors, *Sov. Phys. JETP* **34**, 1144 (1972).
- [52] J. S. Meyer and B. D. Simons, Gap fluctuations in inhomogeneous superconductors, *Phys. Rev. B* **64**, 134516 (2001).
- [53] M. V. Feigel'man and M. A. Skvortsov, Universal broadening of the Bardeen-Cooper-Schrieffer coherence peak of disordered superconducting films, *Phys. Rev. Lett.* **109**, 147002 (2012).
- [54] The coupling between the amplitude and phase fluctuations of the order parameter $\Delta = |\Delta|e^{i\theta}$ vanishes after averaging over disorder in the BCS limit due to the effective particle-hole symmetry [33, 56].
- [55] See Supplemental Material.
- [56] E. Andriyakhina, P. Nosov, S. Raghu, and I. Burmistrov, Quantum fluctuations and multifractally enhanced superconductivity in disordered thin films, *J. Low Temp. Phys.* , 1 (2024).
- [57] A. Klein, D. L. Maslov, and A. V. Chubukov, Hidden and mirage collective modes in two dimensional Fermi liquids, *npj Quantum Materials* **5**, 55 (2020).
- [58] R. L. Willett, R. R. Ruel, M. A. Paalanen, K. W. West, and L. N. Pfeiffer, Enhanced finite-wave-vector conductivity at multiple even-denominator filling factors in two-dimensional electron systems, *Phys. Rev. B* **47**, 7344

(1993).

- [59] R. L. Willett, R. R. Ruel, K. W. West, and L. N. Pfeiffer, Experimental demonstration of a Fermi surface at one-half filling of the lowest Landau level, *Phys. Rev. Lett.* **71**, 3846 (1993).
- [60] P. H. McGuinness, E. Zhakina, M. König, M. D. Bachmann, C. Putzke, P. J. W. Moll, S. Khim, and A. P. Mackenzie, Low-symmetry nonlocal transport in microstructured squares of delafossite metals, *Proceedings of the National Academy of Sciences* **118**, e2113185118 (2021).
- [61] P. Dyke, S. Musolino, H. Kurkjian, D. J. M. Ahmed-Braun, A. Pennings, I. Herrera, S. Hoinka, S. J. J. M. F. Kokkelmans, V. E. Colussi, and C. J. Vale, Higgs oscillations in a unitary Fermi superfluid, *Phys. Rev. Lett.* **132**, 223402 (2024).

End Matter

Appendix A: formula for $\chi_{\text{SH}}^\downarrow(z, \mathbf{q})$. The explicit formula for the function $\chi_{\text{SH}}^\downarrow(z, \mathbf{q})$ is given by

$$\frac{1}{\chi_{\text{SH}}^\downarrow(z, \mathbf{q})} = \begin{cases} [\chi_{\text{SH}}(z, \mathbf{q})]^{-1}, & \text{Im } z > 0 \\ [\chi_{\text{SH}}(z, \mathbf{q})]^{-1} + 2i\rho_{\mathbf{q}}(z), & \text{Im } z \leq 0. \end{cases} \quad (\text{A1})$$

Here $[\chi_{\text{SH}}(z, \mathbf{q})]^{-1}$ is defined in Eq. (5), and $\rho_{\mathbf{q}}(z)$ is the analytic continuation of $\rho_{\mathbf{q}}(\omega)$, given in Eq. (6) for $\Delta\tau \ll 1$ and for arbitrary $\Delta\tau$ in [55], from $\omega \geq 2\Delta$ into the lower complex half-plane.

Appendix B: SH pole for $\Delta\tau \ll 1$. Next, we analytically derive the expression for the pole in the dirty limit. Instead of using our global integral representation in Eq. (A1), we will follow an equivalent route by analytically continuing the approximate expression for $\chi_{\text{SH}}^R(\omega, \mathbf{q})$ (given in Eq. (7) on the real axis at $\omega > 2\Delta$) into the lower half plane, thereby ensuring the smoothness of the resulting function across the cut. After setting the inverse of the r.h.s. of Eq. (7) to zero and treating u as a complex variable, we obtain the following equation $\ln(u^* \bar{q}^2/8) = i\pi(1-u^*)/2$. Its solution is given by $u^* \simeq 2 + 2i[1 - W(4\pi/\bar{q}^2)]/\pi$, where $W(y)$ is the Lambert function defined as a solution of the equation $W \exp W = y$. For $y \gg 1$, we find $W(y) \simeq \ln(y/\ln y)$, and thus we can assume that $W(4\pi/\bar{q}^2) \gg 1$. The resulting behavior near the pole is given by

$$\chi_{\text{SH}}^\downarrow(z, \mathbf{q}) \simeq \frac{Z_{\mathbf{q}}}{z - z_{\mathbf{q}}}, \quad \frac{Z_{\mathbf{q}}}{\Delta} \simeq \frac{4\bar{q}^2}{\pi^2} \left[W\left(\frac{4\pi}{\bar{q}^2}\right) + i\pi \right], \quad (\text{B1})$$

and the position of the pole $z_{\mathbf{q}}$ is given by

$$\frac{z_{\mathbf{q}}}{\Delta} \simeq 2 - \frac{\bar{q}^4}{\pi^2} [W(4\pi/\bar{q}^2) - 1]^2 - \frac{2i\bar{q}^4}{\pi} [W(4\pi/\bar{q}^2) - 1]. \quad (\text{B2})$$

Within the leading logarithmic accuracy, we obtain Eq. (9).

The position of the pole in the complex momentum plane can also be found from Eq. (7). After rewriting

- [62] I. Carusotto and Y. Castin, Atom interferometric detection of the pairing order parameter in a Fermi gas, *Phys. Rev. Lett.* **94**, 223202 (2005).
- [63] M. Endres, T. Fukuhara, D. Pekker, M. Cheneau, P. Schauß, C. Gross, E. Demler, S. Kuhr, and I. Bloch, The ‘Higgs’ amplitude mode at the two-dimensional superfluid/Mott insulator transition, *Nature* **487**, 454 (2012).

the expression in Eq. (7) as

$$\chi_{\text{SH}}^R(\omega, \mathbf{q}) \simeq 2\sqrt{\frac{u^2-1}{\bar{\omega}-2}} \left[\ln \frac{2^4}{\bar{\omega}-2} + u \ln \frac{u-1}{u+1} + i\pi(1-u) \right]^{-1} \quad (\text{B3})$$

for $\omega > 2\Delta$ and $\Delta\tau \ll 1$, setting the inverse of this expression to zero, finding the solution \tilde{u}_* , and converting it back to momentum \bar{q} , we obtain

$$\chi_{\text{SH}}^R(\omega, \mathbf{q}) \simeq \frac{\tilde{Z}_\omega}{\bar{q}^2 - \bar{q}_\omega^2}, \quad \bar{q}_\omega^2 \simeq \frac{2\pi\sqrt{\bar{\omega}-2}}{\ln \frac{2^4}{\bar{\omega}-2}} \left[i + \frac{\pi}{\ln \frac{2^4}{\bar{\omega}-2}} \right], \quad (\text{B4})$$

and $\tilde{Z}_\omega \simeq 1/|\ln((\bar{\omega}-2)^{1/4}/2)|$ is the residue at \bar{q}_ω^2 . Its Fourier transform leads to Eq. (12) and (13) [55].

Appendix C: explicit expressions for the nonlinear current response. The nonlinear current response at $q=0$ was analyzed in [26]. Here, we extend that analysis to finite q . The diagrams determining the paramagnetic contribution to the current are identical to those in [26]. A straightforward calculation yields Eq. (14), where the function $\mathcal{B}_{\text{SH}}^R(\omega, q)$ is expressed as a product of two fermionic loops, each connecting two external vector potential vertices to the SH susceptibility

$$\mathcal{B}_{\text{SH}}^R(\omega, q) = -2\pi B_1^R(\omega, 2q) B_2^R(\omega, 2q), \quad (\text{C1})$$

The expressions for $B_1(\omega_n, q)$ and $B_2(\omega_n, q)$ on the Matsubara axis are given in [55]. Here, we only provide the result after analytic continuation for $\Delta\tau \ll 1$ and at $T = 0$

$$\begin{aligned} \frac{B_1^R(\omega, q)}{\Delta} &= \int_0^\omega \frac{d\varepsilon}{2\pi i} F_{\omega, q}^{RA}(\varepsilon) + \int_{-\infty}^{+\infty} \frac{d\varepsilon}{4\pi i} \text{sgn}(\varepsilon - \omega) F_{\omega, q}^{RR}(\varepsilon), \\ F_{\omega, q}^{Rs}(\varepsilon) &= \frac{\Delta^2 + 3\varepsilon^2 - \omega^2 - E_{\varepsilon+\omega}^R E_{\varepsilon-\omega}^s}{(Dq^2 + E_{\varepsilon+\omega}^R + E_{\varepsilon-\omega}^s) E_{\varepsilon+\omega}^R E_{\varepsilon-\omega}^s}, \\ E_\varepsilon^R &= \theta(\Delta - |\varepsilon|) \sqrt{\Delta^2 - \varepsilon^2} - i\theta(|\varepsilon| - \Delta) \text{sgn}(\varepsilon) \sqrt{\varepsilon^2 - \Delta^2} \end{aligned} \quad (\text{C2})$$

and $E_\varepsilon^A = E_{-\varepsilon}^R$. Similarly, for B_2^R , we find

$$\begin{aligned} \frac{B_2^R(\omega, q)}{\Delta} &= \int_0^\omega \frac{d\varepsilon}{2\pi i} \Phi_{\omega, q}^{RAA}(\varepsilon) + \int_\omega^{2\omega} \frac{d\varepsilon}{2\pi i} \Phi_{\omega, q}^{RRA}(\varepsilon) \\ &+ \int_{-\infty}^{+\infty} \frac{d\varepsilon}{4\pi i} \text{sgn}(\varepsilon - 2\omega) \Phi_{\omega, q}^{RRR}(\varepsilon), \end{aligned} \quad (\text{C3})$$

where we also defined

$$\begin{aligned} \Phi_{\omega, q}^{Rs\sigma}(\varepsilon) &= \frac{1}{(Dq^2 + E_{\varepsilon+\omega}^R + E_{\varepsilon-\omega}^s) E_{\varepsilon+\omega}^R E_{\varepsilon-\omega}^s} \\ &\times \left\{ \left(\frac{1}{E_{\varepsilon+2\omega}^R} + \frac{1}{E_{\varepsilon-2\omega}^\sigma} \right) (\Delta^2 + \varepsilon^2 - \omega^2 - E_{\varepsilon+\omega}^R E_{\varepsilon-\omega}^s) \right. \\ &\left. + 2\varepsilon \left(\frac{\varepsilon + 2\omega}{E_{\varepsilon+2\omega}^R} + \frac{\varepsilon - 2\omega}{E_{\varepsilon-2\omega}^\sigma} \right) \right\}. \end{aligned} \quad (\text{C4})$$

Finally, the quasiparticle contribution, $J_{3\omega, 3q}^{(\text{qp})}$, is given by

$$J_{3\omega, 3q}^{(\text{qp})} = -4\pi\nu D^2 B_3^R(\omega, 2q) |\mathbf{A}_{\omega, \mathbf{q}}|^2 \mathbf{A}_{\omega, \mathbf{q}}, \quad (\text{C5})$$

where $B_3(\omega_n, q)$ on the Matsubara axis is provided in [55]. The real frequency expression for $B_3^R(\omega, q)$ is the same as for $B_2^R(\omega, q)$ in Eq. (C3), but with $\Phi_{\omega, q}^{Rs\sigma}(\varepsilon)$ replaced by $W_{\omega, q}^{Rs\sigma}(\varepsilon)$, where

$$\begin{aligned} W_{\omega, q}^{Rs\sigma}(\varepsilon) &= \frac{1}{(Dq^2 + E_{\varepsilon+\omega}^R + E_{\varepsilon-\omega}^s) E_\varepsilon^R} \left\{ \left(\frac{\Delta}{E_{\varepsilon+2\omega}^R} + \frac{\Delta}{E_{\varepsilon-2\omega}^\sigma} \right) \right. \\ &\times \left(1 + \frac{\omega^2 - \Delta^2 - 3\varepsilon^2}{E_{\varepsilon+\omega}^R E_{\varepsilon-\omega}^s} \right) - \frac{\varepsilon}{\Delta} \left(1 + \frac{3\Delta^2 - \omega^2 + \varepsilon^2}{E_{\varepsilon+\omega}^R E_{\varepsilon-\omega}^s} \right) \\ &\left. \times \left(\frac{\varepsilon + 2\omega}{E_{\varepsilon+2\omega}^R} + \frac{\varepsilon - 2\omega}{E_{\varepsilon-2\omega}^\sigma} \right) \right\}. \end{aligned} \quad (\text{C6})$$

Near the resonance at $\omega \approx \Delta$, we find a logarithmic divergence

$$B_3^R(\omega, q) \approx \frac{1}{\pi} \frac{1}{Dq^2/\Delta + 1 - i\sqrt{3}} \ln \frac{\Delta}{|\omega - \Delta|}. \quad (\text{C7})$$

Therefore, $J_{3\omega_{\text{max}}(q)/2, 3q}^{(\text{qp})}$ increases as $\ln 1/(\xi q)$ for $\xi q \ll 1$. The expressions for arbitrary $\Delta\tau$ can be obtained by replacing factors $(Dq^2 + E_{\varepsilon+\omega}^R + E_{\varepsilon-\omega}^s)^{-1}$ in Eqs. (C2), (C4), (C6) with $S_q(E_{\varepsilon+\omega}^R + E_{\varepsilon-\omega}^s)$.

ONLINE SUPPORTING INFORMATION

Spatially-resolved dynamics of the amplitude Schmid-Higgs mode in disordered superconductors

P. A. Nosov,¹ E. S. Andriyakhina,² and I. S. Burmistrov^{3,4}

¹*Department of Physics, Harvard University, Cambridge, Massachusetts 02138, USA*

²*Freie Universität Berlin, Dahlem Center for Complex Quantum Systems
and Fachbereich Physik, Arnimallee 14, Berlin, 14195, Germany*

³*L.D. Landau Institute for Theoretical Physics, acad. Semenova av.1-a, Chernogolovka, 142432, Russia*

⁴*Laboratory for Condensed Matter Physics, HSE University, Moscow, 101000, Russia*

These notes contain: (i) derivation of the SH susceptibility on the Matsubara axis (Eq. (3) of the main text) and its analytic continuation to the physical Riemann sheet (Eq. (5) of the main text), (ii) derivation of the approximate expression for the retarded SH susceptibility in the dirty limit (Eq. (7) of the main text), (iii) details of the long-distance and late-time asymptotic analysis of the SH response, (iv) analysis of the crossover between the dirty and clean regimes for the SH pole, and (v) additional details of the nonlinear current response calculation.

DERIVATION OF THE SH SUSCEPTIBILITY

The normal and anomalous Matsubara Green's functions of a disordered BCS superconductor can be expressed in the exact eigenbasis defined for a given realization of random potential:

$$G(i\varepsilon_n, \mathbf{r}, \mathbf{r}') = \sum_{\alpha} \varphi_{\alpha}(\mathbf{r})\varphi_{\alpha}(\mathbf{r}') \frac{i\varepsilon_n + \xi_{\alpha}}{\varepsilon_n^2 + \xi_{\alpha}^2 + \Delta^2}, \quad F(i\varepsilon_n, \mathbf{r}, \mathbf{r}') = \sum_{\alpha} \varphi_{\alpha}(\mathbf{r})\varphi_{\alpha}(\mathbf{r}') \frac{\Delta}{\varepsilon_n^2 + \xi_{\alpha}^2 + \Delta^2}, \quad (\text{S1})$$

where $\varepsilon_n = 2\pi T(n+1/2)$, and $\varphi_{\alpha}(\mathbf{r})$ is the exact single particle eigenfunction with the energy ξ_{α} . The mean-field order parameter Δ is determined via the self-consistency condition $\Delta = \lambda_{\text{BCS}} T \sum_m F(\varepsilon_m, \mathbf{r}, \mathbf{r}')/\nu$. The latter, according to the Anderson's theorem [1–3], leads to the standard BCS gap equation

$$1 = \pi \lambda_{\text{BCS}} T \sum_m \frac{1}{\sqrt{\Delta^2 + \varepsilon_m^2}}, \quad (\text{S2})$$

provided that the wave-function amplitude $|\varphi_{\alpha}(\mathbf{r})|^2$ is essentially a non-fluctuating constant set only by normalization. Within the mean-field approach, $\Pi_{\Delta\Delta}$ can be computed as follows

$$\Pi_{\Delta\Delta}(i\omega_n, \mathbf{r}, \mathbf{r}') = \frac{T}{\pi\nu} \sum_m \left\{ G(i\varepsilon_m + i\omega_n, \mathbf{r}, \mathbf{r}') G(-i\varepsilon_m, \mathbf{r}, \mathbf{r}') - F(i\varepsilon_m + i\omega_n, \mathbf{r}, \mathbf{r}') F(-i\varepsilon_m, \mathbf{r}, \mathbf{r}') \right\} \quad (\text{S3})$$

Our first step is to calculate the disorder-averaged Fourier transform of this correlation function

$$\Pi_{\Delta\Delta}(i\omega_n, \mathbf{q}) \equiv \int d^d r' \overline{\Pi_{\Delta\Delta}(i\omega_n, \mathbf{r}, \mathbf{r}')} e^{i\mathbf{q}\cdot(\mathbf{r}-\mathbf{r}')}, \quad (\text{S4})$$

where \overline{A} denotes the average of A over different realizations of disorder. This average can be performed by using the well-known expression for the averaged irreducible dynamical structure factor of single-particle wave-functions in a random potential [4, 5]

$$\int d^d r' e^{i\mathbf{q}\cdot(\mathbf{r}-\mathbf{r}')} \sum_{\alpha\beta} \overline{\varphi_{\alpha}(\mathbf{r})\varphi_{\beta}(\mathbf{r})\varphi_{\alpha}(\mathbf{r}')\varphi_{\beta}(\mathbf{r}')\delta(\xi - \xi_{\alpha})\delta(\xi' - \xi_{\beta})} = \frac{\nu}{2} \left[S_{\mathbf{q}}(i(\xi - \xi')) + S_{\mathbf{q}}(i(\xi' - \xi)) \right]. \quad (\text{S5})$$

Here, $S_{\mathbf{q}}(z)$ is the analytic continuation of the structure factor $S_{\mathbf{q}}(E)$, given in the main text, from real $E>0$ to complex z . In particular, in 2D and 3D we have

$$[S_{\mathbf{q}}^{2\text{D}}(E)]^{-1} = \sqrt{v_F^2 q^2 + (1/\tau + E)^2} - 1/\tau, \quad [S_{\mathbf{q}}^{3\text{D}}(E)]^{-1} = \frac{2iv_F q}{\ln[(1+\tau E + ilq)/(1+\tau E - ilq)]} - 1/\tau. \quad (\text{S6})$$

We emphasize that Eq. (S5) and Eq. (S6) are well-justified in the diffusive limit $E_F \tau \gg 1$ and $q \ll l$, where $l = v_F \tau$ is the mean free path, v_F is the Fermi velocity, τ is the mean free time, and E_F is the Fermi energy. Diagrammatically,

this expression corresponds to the summation of the ladder-type corrections to the particle-hole and particle-particle propagators [6, 7]. As clearly seen from Eq. (S6), $S_{\mathbf{q}}(iz)$ is analytic in the lower half-plane of z , whereas $S_{\mathbf{q}}(-iz)$ is analytic in the upper half-plane.

After substituting Eq. (S1) into Eq. (S3), and using Eq. (S5) in combination with additional unity insertions $1 = \int d\xi \delta(\xi - \xi_\alpha)$ under the sum, we obtain

$$\Pi_{\Delta\Delta}(i\omega_n, \mathbf{q}) = \frac{T}{2\pi} \sum_m \int_{-\infty}^{\infty} d\xi d\xi' \frac{(i\varepsilon_m + i\omega_n + \xi)(-i\varepsilon_m + \xi') - \Delta^2}{((\varepsilon_m + \omega_n)^2 + \xi^2 + \Delta^2)(\varepsilon_m^2 + \xi'^2 + \Delta^2)} \left[S_{\mathbf{q}}(i(\xi - \xi')) + S_{\mathbf{q}}(i(\xi' - \xi)) \right]. \quad (\text{S7})$$

Let us first integrate over ξ . The poles of the prefactor are at $\xi = \pm iE_{\varepsilon_m + \omega_n}$, where $E_\xi = \sqrt{\xi^2 + \Delta^2}$. The first (second) term in square brackets has its non-analyticities at $\text{Im } \xi > 0$ ($\text{Im } \xi < 0$). Thus, for the first term we can close the contour of integration in the lower half-plane of ξ and pick up the residue at $\xi = -iE_{\varepsilon_m + \omega_n}$, and for the second term we close the contour in the upper half-plane. The remaining integral over ξ' can be done in the same way. We thus arrive at the following expression

$$\Pi_{\Delta\Delta}(i\omega_n, \mathbf{q}) = \pi T \sum_m S_{\mathbf{q}}(E_{\varepsilon_m} + E_{\varepsilon_m + \omega_n}) \left[1 + \frac{\varepsilon_m(\varepsilon_m + \omega_n) - \Delta^2}{E_{\varepsilon_m} E_{\varepsilon_m + \omega_n}} \right]. \quad (\text{S8})$$

After combining the definition of the inverse SH susceptibility (Eq. (2) from the main text), our result in Eq. (S8), and the gap equation Eq. (S2), we finally arrive at

$$\frac{1}{\chi_{\text{SH}}(i\omega_n, \mathbf{q})} = \pi T \sum_m \left\{ \frac{1}{E_{\varepsilon_m}} - S_{\mathbf{q}}(E_{\varepsilon_m} + E_{\varepsilon_m + |\omega_n|}) \left[1 + \frac{\varepsilon_m(\varepsilon_m + |\omega_n|) - \Delta^2}{E_{\varepsilon_m} E_{\varepsilon_m + |\omega_n|}} \right] \right\}, \quad (\text{S9})$$

where we also replaced ω_n with $|\omega_n|$ because the sum is an even function of ω_n . Eq. (S9) is Eq. (2) of the main text. At $q = 0$ and $T = 0$, this expression reduces to

$$\frac{1}{\chi_{\text{SH}}(i\omega_n, 0)} = \frac{\sqrt{4\Delta^2 + \omega_n^2}}{2|\omega_n|} \ln \left(\frac{\sqrt{4\Delta^2 + \omega_n^2} + |\omega_n|}{\sqrt{4\Delta^2 + \omega_n^2} - |\omega_n|} \right). \quad (\text{S10})$$

We note that, strictly speaking, the r.h.s. in Eq. (S9) is the disorder-averaged inverse SH susceptibility, and not the inverse of the averaged SH susceptibility. However, the difference is a small correction of higher order in $1/E_F\tau \ll 1$ which can be safely neglected [7].

Analytic continuation on the physical Riemann sheet

Our next task is to analytically continue Eq. (S9) into a complex frequency plane on the physical Riemann sheet. First, we establish the relation between the desired analytic continuation $\chi_{\text{SH}}(z, \mathbf{q})$ and the retarded function $\chi_{\text{SH}}^R(\varepsilon, \mathbf{q}) \equiv \chi_{\text{SH}}(\varepsilon + i0^+, \mathbf{q})$ defined slightly above the real axis. Let us consider the following identity

$$\frac{1}{\chi_{\text{SH}}(i\omega_n, \mathbf{q})} = \int_{\mathcal{C}} \frac{dz}{2\pi i} \frac{[\chi_{\text{SH}}(z, \mathbf{q})]^{-1}}{z - i\omega_n}, \quad (\text{S11})$$

where \mathcal{C} is a small closed contour encircling $i\omega_n$, and $\omega_n \geq 0$. As guaranteed by causality, the desired analytic continuation $[\chi_{\text{SH}}(z, \mathbf{q})]^{-1}$ is analytic in the upper half-plane $\text{Im } z > 0$. Thus, we can extend the contour to go slightly above the real axis from $-\Lambda + i0^+$ to $+\Lambda + i0^+$, $\Lambda \rightarrow +\infty$, and close it in the upper half-plane

$$\frac{1}{\chi_{\text{SH}}(i\omega_n, \mathbf{q})} = \lim_{\Lambda \rightarrow +\infty} \left\{ \int_{-\Lambda}^{+\Lambda} \frac{d\varepsilon}{2\pi i} \frac{[\chi_{\text{SH}}^R(\varepsilon, \mathbf{q})]^{-1}}{\varepsilon - i\omega_n} + \frac{\Lambda}{2\pi} \int_0^\pi d\theta \frac{e^{i\theta} [\chi_{\text{SH}}(\Lambda e^{i\theta}, \mathbf{q})]^{-1}}{\Lambda e^{i\theta} - i\omega_n} \right\}. \quad (\text{S12})$$

Normally, the second term vanishes in the limit $\Lambda \rightarrow \infty$, whereas the first term is finite and leads to the usual Kramers–Kronig-type relation. Here this is not the case: as one can see from Eq. (S10), $1/|\chi_{\text{SH}}(i\omega_n, \mathbf{q})|$ is a growing

function on the Matsubara axis. As a consequence, both terms in Eq. (S12) diverge logarithmically. However, as we will see, their divergencies exactly compensate each other. Let us consider the second integral and approximate it as

$$\frac{\Lambda}{2\pi} \int_0^\pi d\theta \frac{e^{i\theta} [\chi_{\text{SH}}(\Lambda e^{i\theta}, \mathbf{q})]^{-1}}{\Lambda e^{i\theta} - i\omega_n} \approx \frac{1}{2\pi} \int_0^\pi d\theta [\chi_{\text{SH}}(\Lambda e^{i\theta}, \mathbf{q})]^{-1} + \mathcal{O}(\Lambda^{-1}). \quad (\text{S13})$$

Next, we can use the fact that the SH susceptibility becomes momentum-independent at large complex frequencies, so we can directly use the $q = 0$ expression in Eq. (S10)

$$[\chi_{\text{SH}}(z = \Lambda e^{i\theta}, \mathbf{q})]^{-1} \approx [\chi_{\text{SH}}(z = \Lambda e^{i\theta}, 0)]^{-1} = \frac{i\sqrt{4\Delta^2 - z^2}}{2z} \ln \left(\frac{\sqrt{4\Delta^2 - z^2} - iz}{\sqrt{4\Delta^2 - z^2} + iz} \right) = -\frac{i\pi}{2} + i\theta + \ln \frac{\Lambda}{\Delta} + \mathcal{O}(\Lambda^{-1}). \quad (\text{S14})$$

After integrating over θ and replacing $\ln \Lambda/\Delta$ with the integral $\frac{1}{2} \int_{-\Lambda}^{\Lambda} d\varepsilon \frac{\theta(|\varepsilon| - 2\Delta)}{\sqrt{\varepsilon^2 - 4\Delta^2}}$ (up to small corrections vanishing in the limit $\Lambda \rightarrow \infty$), we obtain

$$\frac{1}{\chi_{\text{SH}}(i\omega_n, \mathbf{q})} = \int_{-\infty}^{+\infty} \frac{d\varepsilon}{2\pi} \left\{ \frac{\pi \theta(|\varepsilon| - 2\Delta)}{2\sqrt{\varepsilon^2 - 4\Delta^2}} - \frac{i[\chi_{\text{SH}}^R(\varepsilon, \mathbf{q})]^{-1}}{\varepsilon - i\omega_n} \right\}, \quad \omega_n \geq 0. \quad (\text{S15})$$

If $i\omega_n$ is continued to complex frequency z , then the integral on the r.h.s. of the expression above gives $1/\chi_{\text{SH}}(z, \mathbf{q})$ if $\text{Im } z > 0$, and zero if $\text{Im } z < 0$ (this is evident from the r.h.s. of Eq. (S11) - the only non-analyticity of the integrand at z leaves the area that could be enclosed by \mathcal{C} without crossing the branch cut on the real axis). Evidently, since $\chi_{\text{SH}}(i\omega_n, \mathbf{q}) = \chi_{\text{SH}}(-i|\omega_n|, \mathbf{q}) = \chi_{\text{SH}}(i|\omega_n|, \mathbf{q})$ for $\omega_n < 0$, we also have the following representation

$$\frac{1}{\chi_{\text{SH}}(i\omega_n, \mathbf{q})} = \int_{-\infty}^{+\infty} \frac{d\varepsilon}{2\pi} \left\{ \frac{\pi \theta(|\varepsilon| - 2\Delta)}{2\sqrt{\varepsilon^2 - 4\Delta^2}} - \frac{i[\chi_{\text{SH}}^R(\varepsilon, \mathbf{q})]^{-1}}{\varepsilon + i\omega_n} \right\}, \quad \omega_n < 0. \quad (\text{S16})$$

We again notice that after $i\omega_n$ is replaced with z , the integral on the r.h.s. is identical to $1/\chi_{\text{SH}}(z, \mathbf{q})$ if $\text{Im } z < 0$, and produces zero if $\text{Im } z > 0$. Thus, the integral representation of $1/\chi_{\text{SH}}(z, \mathbf{q})$ in the entire complex plane (except for the branch cuts on the real axis) is given by the sum of integrals on the r.h.s. of Eq. (S15) and Eq. (S16) with $i\omega_n$ replaced by z

$$\frac{1}{\chi_{\text{SH}}(z, \mathbf{q})} = \int_{-\infty}^{+\infty} \frac{d\varepsilon}{2\pi} \left\{ \frac{\pi \theta(|\varepsilon| - 2\Delta)}{\sqrt{\varepsilon^2 - 4\Delta^2}} - \frac{i[\chi_{\text{SH}}^R(\varepsilon, \mathbf{q})]^{-1}}{\varepsilon - z} - \frac{i[\chi_{\text{SH}}^R(\varepsilon, \mathbf{q})]^{-1}}{\varepsilon + z} \right\} = \int_{-\infty}^{+\infty} \frac{d\varepsilon}{\pi} \left\{ \frac{\text{Im}[\chi_{\text{SH}}^R(\varepsilon, \mathbf{q})]^{-1}}{\varepsilon - z} + \frac{\pi \theta(|\varepsilon| - 2\Delta)}{2\sqrt{\varepsilon^2 - 4\Delta^2}} \right\} \quad (\text{S17})$$

where we used the fact that the real (imaginary) part of $[\chi_{\text{SH}}^R(\varepsilon, \mathbf{q})]^{-1}$ is even (odd). After rewriting $\text{Im}[\chi_{\text{SH}}^R(\varepsilon, \mathbf{q})]^{-1}$ via the spectral density $\rho_{\mathbf{q}}(\varepsilon)$ as $\text{Im}[\chi_{\text{SH}}^R(\varepsilon, \mathbf{q})]^{-1} = \text{sgn}(\varepsilon)\theta(|\varepsilon| - 2\Delta)\rho_{\mathbf{q}}(|\varepsilon|)$, we arrive at Eq. (5) of the main text.

The remaining step is to calculate $\text{Im}[\chi_{\text{SH}}^R(\varepsilon, \mathbf{q})]^{-1}$ at $T = 0$. In principle, this can be done directly from (S9) by transforming the sum into a real-frequency integral involving the Fermi-Dirac distribution. Next, $i\omega_n$ is replaced by $\omega + i0^+$, and the imaginary part is taken at $T = 0$. Here we take a slightly different route and start with Eq. (S7). After replacing the sum with an integral, we find

$$\Pi_{\Delta\Delta}(i\omega_n, \mathbf{q}) = \frac{1}{\pi} \int_{-\infty}^{\infty} d\xi d\xi' \text{Re} \{S_{\mathbf{q}}(i(\xi - \xi'))\} \int_{\mathcal{C}} \frac{dz}{4\pi i} \mathcal{F}(z) \frac{(z + i\omega_n + \xi)(\xi' - z) - \Delta^2}{(\xi^2 + \Delta^2 - (z + i\omega_n)^2)(\xi'^2 + \Delta^2 - z^2)}, \quad (\text{S18})$$

where $\mathcal{F}(z) = \tanh(z/2T)$, and the contour \mathcal{C} consists of small circles enclosing only the poles at $z = i\varepsilon_m$ for $m \in \mathbb{Z}$. The other poles of the integrand are at $\pm E_{\xi'}$ and $-i\omega_n \pm E_{\xi}$. After deforming the contour to infinity, we pick up the contributions from these poles, and find

$$\Pi_{\Delta\Delta}(i\omega_n, \mathbf{q}) = \sum_{\eta=\pm} \int_{-\infty}^{\infty} \frac{d\xi d\xi'}{4\pi} \text{Re} \{S_{\mathbf{q}}(i(\xi - \xi'))\} \mathcal{F}(E_{\xi}) \frac{(i\omega_n + \xi' - \eta E_{\xi})(\xi + \eta E_{\xi}) - \Delta^2}{E_{\xi} E_{\xi'}} \left[\frac{1}{i\omega_n - \eta E_{\xi} + E_{\xi'}} - \frac{1}{i\omega_n - \eta E_{\xi} - E_{\xi'}} \right]. \quad (\text{S19})$$

Here we used $\mathcal{F}(E - i\eta\omega_n) = \mathcal{F}(E)$, $\mathcal{F}(-E) = \mathcal{F}(E)$, and interchanged the integration variables $\xi \leftrightarrow \xi'$ in one of the terms. For further convenience, we can use the following identity

$$1 = \int_{\Delta}^{+\infty} dE \delta(E - E_\varepsilon) = \int_{\Delta}^{+\infty} dE \sum_{s=\pm} \frac{E}{\sqrt{E^2 - \Delta^2}} \delta(\varepsilon + s\sqrt{E^2 - \Delta^2}) \quad (\text{S20})$$

in order to eliminate the integrals over ξ, ξ' . After setting $T=0$ and taking the imaginary part of the resulting expression, we find

$$\begin{aligned} \text{Im} \Pi_{\Delta\Delta}^R(\omega, \mathbf{q}) &= \frac{1}{2} \sum_{\eta=\pm} \int_{\Delta}^{+\infty} dE dE' \left[\eta + \frac{E(|\omega| - E) - \Delta^2}{\sqrt{E^2 - \Delta^2} \sqrt{E'^2 - \Delta^2}} \right] (\delta(\omega - E - E') - \delta(\omega + E + E')) \\ &\times \text{Re} S_{\mathbf{q}}(i(\sqrt{E^2 - \Delta^2} - \eta\sqrt{E'^2 - \Delta^2})). \end{aligned} \quad (\text{S21})$$

The final result reads as

$$\begin{aligned} \text{Im}[\chi_{\text{SH}}^R(\omega, \mathbf{q})]^{-1} &= -\frac{1}{2} \text{sgn}(\omega) \theta(|\omega| - 2\Delta) \sum_{\eta=\pm} \int_{\Delta}^{|\omega| - \Delta} dE \left[\eta + \frac{E(|\omega| - E) - \Delta^2}{\sqrt{E^2 - \Delta^2} \sqrt{(|\omega| - E)^2 - \Delta^2}} \right] \\ &\times \text{Re} S_{\mathbf{q}}(i(\sqrt{E^2 - \Delta^2} - \eta\sqrt{(|\omega| - E)^2 - \Delta^2})). \end{aligned} \quad (\text{S22})$$

This expression is valid for arbitrary $\Delta\tau$. In the dirty limit, $\Delta\tau \ll 1$, the integral can be done analytically in terms of Elliptic functions, and the result is given in Eq. (6) of the main text.

Let us now demonstrate that Eq. (S22) reproduces the correct answer in the clean limit $1/\tau = 0$, in particular in two dimensions [8]. After setting $1/\tau$ to zero in Eq. (S6), or evaluating Eq. (S5) directly by replacing random wavefunctions with plane waves, we find $\text{Re} S_{\mathbf{q}}(ix) = \theta(v_F q - |x|) / \sqrt{v_F^2 q^2 - x^2}$. We substitute this expression in Eq. (S22) and expand the integrand in powers of $v_F q / \Delta \ll 1$ and $(\omega/\Delta - 2) \ll 1$ while keeping the ratio $4\Delta^2(\omega/\Delta - 2)/(v_F^2 q^2) = \zeta$ fixed. For $\zeta < 1$, the step-function in Eq. (S22) equals to one for all E , and we obtain

$$\text{Im}[\chi_{\text{SH}}^R(\omega, \mathbf{q})]^{-1} = -\frac{v_F q}{2\Delta} \sqrt{\zeta} \text{Re} E \left(\frac{1}{\sqrt{\zeta + i0^+}} \right), \quad \omega > 2\Delta, \quad (\text{S23})$$

where $0 < \zeta < 1$, and $E(x) = \int_0^{\pi/2} d\theta \sqrt{1 - x^2 \sin^2 \theta}$. Eq. (S23) agrees with Eq. (21) in [8].

REAL PART OF χ_{SH}^R IN THE DIRTY LIMIT $\Delta\tau \ll 1$

As was explained in the main text, the behavior of $\text{Im} 1/\chi_{\text{SH}}^R(\omega, \mathbf{q})$ for $\Delta\tau \ll 1$ and in the long-wavelength limit $\xi q \ll 1$, $|\omega - 2\Delta|/\Delta \ll 1$ with $|\omega/\Delta - 2|/\xi^4 q^4$ fixed can be easily obtained by expanding our full analytic result in Eq. (6) of the main text. The real part of $1/\chi_{\text{SH}}^R(\omega, \mathbf{q})$ is given by the principle value of the integral

$$\text{Re}[\chi_{\text{SH}}^R(\omega, \mathbf{q})]^{-1} = \int_{-\infty}^{+\infty} \frac{d\varepsilon}{\pi} \left\{ \frac{\text{Im}[\chi_{\text{SH}}^R(\varepsilon, \mathbf{q})]^{-1}}{\varepsilon - \omega} + \frac{\pi \theta(|\varepsilon| - 2\Delta)}{2\sqrt{\varepsilon^2 - 4\Delta^2}} \right\}. \quad (\text{S24})$$

This integral can be computed in two steps. First, we notice that $\text{Re}[\chi_{\text{SH}}^R(2\Delta + 0^+, 0)]^{-1} = 0$. This is most easily seen directly from Eq. (S10). Alternatively, one can take the $q=0$ limit in Eq. (6) of the main text, yielding $\text{Im}[\chi_{\text{SH}}^R(\omega, 0)]^{-1} = -\text{sgn}(\omega) \theta(|\omega| - 2\Delta) \pi \sqrt{\omega^2 - 4\Delta^2} / (2|\omega|)$ for any ω , and perform the integral in Eq. (S24) directly. Thus, we can expand Eq. (S24) by formally adding and subtracting $\text{Re}[\chi_{\text{SH}}^R(2\Delta, 0)]^{-1}$ from the r.h.s., integrating by parts, and evaluating the remaining integral with logarithmic accuracy using $\text{Im}[\chi_{\text{SH}}^R(\omega, \mathbf{q})]^{-1} \simeq \pi(\xi^2 q^2 - \sqrt{\xi^4 q^4 + 4(\omega/\Delta - 2)})/4$, we find

$$\begin{aligned} \text{Re}[\chi_{\text{SH}}^R(2\Delta, \mathbf{q})]^{-1} &= \frac{2}{\pi} \int_{2\Delta}^{\infty} d\varepsilon \frac{\varepsilon \text{Im}([\chi_{\text{SH}}^R(\varepsilon, \mathbf{q})]^{-1} - [\chi_{\text{SH}}^R(\varepsilon, 0)]^{-1})}{\varepsilon^2 - 4\Delta^2} = \frac{1}{\pi} \text{Im} \left([\chi_{\text{SH}}^R(\varepsilon, \mathbf{q})]^{-1} - [\chi_{\text{SH}}^R(\varepsilon, 0)]^{-1} \right) \ln \frac{\varepsilon^2 - 4\Delta^2}{4\Delta^2} \Bigg|_{\varepsilon=2\Delta}^{\infty} \\ &- \frac{1}{\pi} \int_{2\Delta}^{\infty} d\varepsilon \ln \frac{\varepsilon^2 - 4\Delta^2}{4\Delta^2} \partial_\varepsilon \text{Im}([\chi_{\text{SH}}^R(\varepsilon, \mathbf{q})]^{-1} - [\chi_{\text{SH}}^R(\varepsilon, 0)]^{-1}) \simeq \int_0^{\infty} \frac{d\delta}{4} \left[\frac{1}{\sqrt{\xi^4 q^4/4 + \delta}} - \frac{1}{\sqrt{\delta}} \right] \ln \delta = \xi^2 q^2 \ln \frac{e^{1/2}}{\xi q}. \end{aligned} \quad (\text{S25})$$

In the first line here we used the fact that the imaginary part saturates to a constant at large frequency, independent of momentum. Our simple estimation in Eq. (S25) is not sufficient to fully determine the numerical factor under the logarithm. A slightly more careful calculation of the sub-leading term can be done as follows: we first subtract the leading order result $\xi^2 q^2 \ln \frac{e^{1/2}}{\xi q} \equiv \int_0^\infty \frac{d\delta}{4} [(\xi^4 q^4/4 + \delta)^{-1/2} - \delta^{-1/2}] \ln \delta$ from both sides of the exact relation

$$\text{Re}[\chi_{\text{SH}}^R(2\Delta, \mathbf{q})]^{-1} = -\frac{1}{\pi} \int_0^\infty d\delta \ln[\delta(1 + \delta/4)] \partial_\delta \text{Im} \left([\chi_{\text{SH}}^R(2\Delta + \Delta\delta, \mathbf{q})]^{-1} - [\chi_{\text{SH}}^R(2\Delta + \Delta\delta, 0)]^{-1} \right). \quad (\text{S26})$$

Then we differentiate both sides with respect to $\xi^2 q^2$ and take the limit $q \rightarrow 0$. The resulting expression gives us the coefficient \tilde{c} in the expansion $\text{Re}[\chi_{\text{SH}}^R(2\Delta, \mathbf{q})]^{-1} \approx \xi^2 q^2 \ln \frac{e^{1/2}}{\xi q} + \tilde{c} \xi^2 q^2 + \mathcal{O}(\xi^4 q^4)$ as

$$\tilde{c} = \frac{1}{\pi} \int_0^{+\infty} \frac{d\delta \ln[\delta(1 + \delta/4)]}{\delta(\delta + 2)^3(\delta + 4)} \left\{ (\delta + 4)(\delta(\delta + 4) - 4) E \left(\frac{\delta}{\delta + 4} \right) - 4(\delta^2 - 4) K \left(\frac{\delta}{\delta + 4} \right) \right\} = \ln 2 - \frac{1}{2}. \quad (\text{S27})$$

Note that in our notation $E(x) = \int_0^{\pi/2} d\theta \sqrt{1 - x^2 \sin^2 \theta}$. Therefore, we finally obtain

$$\text{Re}[\chi_{\text{SH}}^R(2\Delta, \mathbf{q})]^{-1} = \xi^2 q^2 \ln \frac{2}{\xi q} + \mathcal{O}(\xi^4 q^4). \quad (\text{S28})$$

The frequency dependence for $\omega > 2\Delta$ can be now obtained in a similar way: we add and subtract $\text{Re}[\chi_{\text{SH}}^R(2\Delta, \mathbf{q})]^{-1}$ from the r.h.s. of Eq. (S24), and once more use the asymptotic expression for $\text{Im}[\chi_{\text{SH}}^R(\varepsilon, \mathbf{q})]^{-1}$ given above. The result of this integration is given in Eq. (7) in the main text.

LATE-TIME SH RESPONSE AT FIXED MOMENTUM

Let us consider the FT of the retarded SH susceptibility

$$\chi_{\text{SH}}^R(t, \mathbf{q}) = \int_{-\infty}^{+\infty} \frac{d\omega}{2\pi} e^{-i\omega t} \chi_{\text{SH}}^R(\omega, \mathbf{q}), \quad (\text{S29})$$

for $t > 0$. Given that $\chi_{\text{SH}}(z, \mathbf{q})$ has only branch cuts on the physical sheet, we can rewrite the integral as follows

$$\chi_{\text{SH}}^R(t, \mathbf{q}) = \frac{2}{\pi} \int_{2\Delta}^{+\infty} d\omega \sin(\omega t) \text{Im} \chi_{\text{SH}}^R(\omega, \mathbf{q}) = -\frac{1}{\pi} \text{Re} \int_{2\Delta}^{+\infty} d\omega (e^{i\omega t} - e^{-i\omega t}) \chi_{\text{SH}}^R(\omega, \mathbf{q}). \quad (\text{S30})$$

For the first term, we can rotate the contour of integration counter-clockwise by $\pi/2$ into the upper half-plane. Clearly, this is allowed because $\chi_{\text{SH}}(z)$ does not contain non-analyticities there, and it does not grow exponentially. For the second term, we can rotate the contour clockwise by $\pi/2$ into the unphysical Riemann sheet where the appropriate analytic continuation, $\chi_{\text{SH}}^\downarrow(z)$, is used. As a result, we obtain

$$\chi_{\text{SH}}^R(t, \mathbf{q}) = \text{Im} \left\{ e^{2i\Delta t} \int_0^{+\infty} \frac{dy}{\pi} e^{-ty} \chi_{\text{SH}}(2\Delta + iy, \mathbf{q}) + e^{-2i\Delta t} \int_0^{+\infty} \frac{dy}{\pi} e^{-ty} \chi_{\text{SH}}^\downarrow(2\Delta - iy, \mathbf{q}) \right\} + 2 \text{Im} [Z_{\mathbf{q}} e^{-i\omega_{\mathbf{q}} t}] \theta(\text{Re} \omega_{\mathbf{q}} - 2\Delta). \quad (\text{S31})$$

The second term here corresponds to the possibility of encountering a pole with complex frequency $\omega_{\mathbf{q}}$ on the unphysical sheet while rotating the contour. The first term can be estimated by expanding $\chi_{\text{SH}}(2\Delta + iy)$ and $\chi_{\text{SH}}^\downarrow(2\Delta - iy)$ in powers of y . By construction, $\chi_{\text{SH}}(2\Delta, \mathbf{q}) = \chi_{\text{SH}}^\downarrow(2\Delta, \mathbf{q})$ and real, and thus, the $\sim 1/t$ term vanishes. On the other hand, we have

$$\lim_{y \rightarrow 0^+} \partial_y \chi_{\text{SH}}^\downarrow(2\Delta - iy, \mathbf{q}) = \lim_{\substack{y \rightarrow 0^+ \\ \omega \rightarrow 2\Delta^+}} \partial_y \chi_{\text{SH}}^\downarrow(\omega - iy, \mathbf{q}) = -i \lim_{\omega \rightarrow 2\Delta^+} \partial_\omega \chi_{\text{SH}}^\downarrow(\omega, \mathbf{q}) = -i \lim_{\omega \rightarrow 2\Delta^+} \partial_\omega \chi_{\text{SH}}^R(\omega, \mathbf{q}). \quad (\text{S32})$$

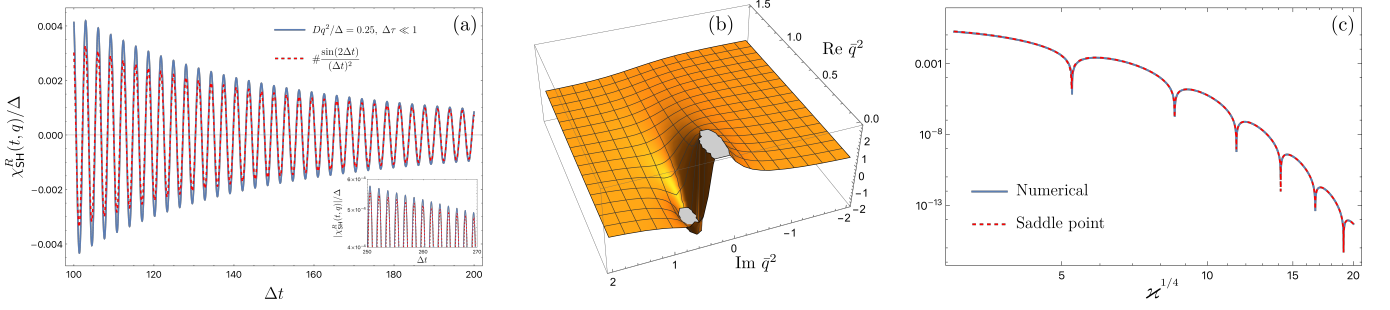


FIG. S1. (a) Oscillations of $\chi_{\text{SH}}^R(t, \mathbf{q})$ in the time domain for $Dq^2/\Delta = 0.25$ ($\xi q = 0.5$), in a dirty limit $\Delta\tau \ll 1$. The red dashed line is the approximation with the first term of Eq. (S33), where the derivative is evaluated numerically without any fitting parameters. The inset is $|\chi_{\text{SH}}^R(t, \mathbf{q})|/\Delta$ on a log-log scale. The decay $\sim 1/t^2$ and the frequency of oscillations 2Δ are clearly seen. (b) Imaginary part of $\chi_{\text{SH}}^R(\omega, \mathbf{q})$ as a function of complex \bar{q}^2 for $\omega/\Delta = 2.2$. (c) Solid blue curve shows the absolute value of the l.h.s. of Eq. (S44) for $\Delta t = 16.5$, as a function of \varkappa . The red dashed curve is the approximation shown on the r.h.s. of Eq. (S44).

In the same way, we find $\lim_{y \rightarrow 0^+} \partial_y \chi_{\text{SH}}(2\Delta + iy, \mathbf{q}) = i \lim_{\omega \rightarrow 2\Delta^+} \partial_\omega \chi_{\text{SH}}^R(\omega, \mathbf{q})$, and thus

$$\chi_{\text{SH}}^R(t, \mathbf{q}) \approx -\frac{2 \sin(2\Delta t)}{\pi t^2} \lim_{\omega \rightarrow 2\Delta^+} \partial_\omega \text{Im} \chi_{\text{SH}}^R(\omega, \mathbf{q}) + 2 \text{Im} [Z_{\mathbf{q}} e^{-i\omega_{\mathbf{q}} t}] \theta(\text{Re} \omega_{\mathbf{q}} - 2\Delta), \quad (\text{S33})$$

This result is given in Eq. (10) of the main text. We note that Eq. (S33) is general and does not require the dirty limit $\Delta\tau \ll 1$. The only details needed are the characteristics of the pole ($\omega_{\mathbf{q}}$, $Z_{\mathbf{q}}$), and the derivative of the imaginary part of χ^R at 2Δ . Note that the first term in Eq. (S33) is exactly what one would obtain by integrating Eq. (S30) by parts twice. The second term, however, would be missed this way. The agreement between Eq. (S33) and the numerical result is shown in Fig. S1(a).

LONG-DISTANCE SH RESPONSE AT FIXED FREQUENCY

We consider the following FT transform

$$\chi_{\text{SH}}^R(\omega, \mathbf{r}) = \int \frac{d^d q}{(2\pi)^d} e^{i\mathbf{q}\cdot\mathbf{r}} \chi_{\text{SH}}^R(\omega, \mathbf{q}), \quad (\text{S34})$$

for $\omega > 0$. For simplicity, let us consider a $d = 3$ case. The integral over the angles is trivial and leads to

$$\chi_{\text{SH}}^R(\omega, \mathbf{r}) = \frac{1}{2\pi^2 r} \int_0^{+\infty} dq q \sin(qr) \chi_{\text{SH}}^R(\omega, q) = -\frac{i}{8\pi^2 r \xi^2} \int_0^{+\infty} d(\bar{q}^2) (e^{i\bar{q}\bar{r}} - e^{-i\bar{q}\bar{r}}) \chi_{\text{SH}}^R(\omega, \bar{q}). \quad (\text{S35})$$

Here we are using the same notation as in the main text: $\bar{q} = \xi q$, and $\bar{r} = r/\xi$. In order to extract the leading oscillatory contribution to this integral, we need to investigate the behavior of $\chi_{\text{SH}}^R(\omega, \bar{q})$ in the complex plane of \bar{q} . We note that χ_{SH}^R is a function of \bar{q}^2 only, so we will promote \bar{q}^2 to a complex variable. Numerical evaluation suggests that χ_{SH}^R has a pole $\bar{q}^2 = \bar{q}_\omega^2$ in the upper half-plane of \bar{q}^2 , i.e. $\text{Re} \bar{q}_\omega^2 > 0$ and $\text{Im} \bar{q}_\omega^2 > 0$ provided $\omega > 2\Delta$, see Fig. S1(b). Moreover, there are no other non-analyticities in the half-plane $\text{Re} \bar{q}^2 > 0$. The properties of this pole in the dirty limit $\Delta\tau \ll 1$ are discussed in End Matter (see Eq. (B4)).

This analytic structure suggests rotating the contours of integration to the imaginary axis in the complex \bar{q}^2 -plane so that in the first term in Eq. (S35) we have $\bar{q}^2 = \rho e^{i\pi/2}$, and $\bar{q}^2 = \rho e^{-i\pi/2}$ in the second term. This results in

$$\chi_{\text{SH}}^R(\omega, \mathbf{r}) = \frac{1}{4\pi^2 r \xi^2} \int_0^{+\infty} d\rho e^{-\bar{r}\sqrt{\rho/2}} \text{Re} \left\{ e^{i\bar{r}\sqrt{\rho/2}} \chi_{\text{SH}}^R(\omega, \bar{q}^2 \rightarrow i\rho) \right\} + \frac{\tilde{Z}_\omega}{4\pi r \xi^2} e^{i\bar{q}_\omega \bar{r}} \theta(\text{Re} \bar{q}_\omega^2), \quad (\text{S36})$$

where the last term originates from the pole. First, we note that the first term in Eq. (S36) is purely real, and thus, $\text{Im} \chi_{\text{SH}}^R(\omega, \mathbf{r})$ only has a contribution from the pole. Next, if we expand $\chi_{\text{SH}}^R(\omega, \bar{q}^2 \rightarrow i\rho)$ in the first term in Eq. (S36)

in powers of ρ and integrate term by term, then we find that all terms in the series vanish identically. From numerical analysis, we find that the first term decays as $\sim 1/r^3$ and contains no oscillations. Thus, the full asymptotic expression reads as

$$\chi_{\text{SH}}^R(\omega, \mathbf{r}) \approx \frac{\tilde{Z}_\omega}{4\pi r \xi^2} e^{iq_\omega \bar{r}} \theta(\text{Re } \bar{q}_\omega^2) + \mathcal{O}(1/r^3, \text{ non-oscillatory}). \quad (\text{S37})$$

We emphasize that this expression is valid in 3D for arbitrary $\Delta\tau$. In the dirty limit $\Delta\tau \ll 1$, we can use Eq. (B4) in End Matter and obtain

$$\text{Im } \chi_{\text{SH}}^R(\omega, \mathbf{r}) \simeq \frac{\sin(r/\xi_\omega) e^{-\frac{r}{\xi_\omega}}}{\pi r \xi^2 \ln \frac{2^4}{\bar{\omega}-2}}, \quad \frac{\xi_\omega}{\xi} = \frac{\ln^{1/2} \frac{2^4}{\bar{\omega}-2}}{\sqrt{\pi}(\bar{\omega}-2)^{1/4}}. \quad (\text{S38})$$

At $\omega = 2\Delta$, one can evaluate the integral directly as follows

$$\chi_{\text{SH}}^R(\omega = 2\Delta, \mathbf{r}) \approx \frac{1}{2\pi^2 r \xi^2} \int_0^{+\infty} dq \frac{\sin(qr)}{q \ln \frac{2}{\xi q}} \approx \frac{1}{4\pi r \xi^2 \ln \frac{2r}{\xi}}, \quad d = 3. \quad (\text{S39})$$

Note that Eq. (S38) and Eq. (S39) smoothly connect at $r \approx \xi_\omega$. Thus, Eq. (S38) describes the oscillatory asymptotic at $r \gg \xi_\omega$ which becomes Eq. (S39) in the range $\xi \ll r \ll \xi_\omega$.

The analysis of the 2D case is similar. The only difference is that the Bessel function $J_0(qr)$ should be used instead of $\sin(qr)/qr$ in Eq. (S35). Consequently, the Bessel function is decomposed as a sum of the Hankel functions $H_0^{(1/2)}(x)$ of the first and second kind. One then can use the fact that $H_0^{(1/2)}(x)$ decays in the first (fourth) quadrant of the complex plane, enabling rotations of the integration contours as in the 3D case. The result in the dirty limit is given in Eq. (12) of the main text.

LATE-TIME AND LONG-DISTANCE SH RESPONSE

Finally, let us consider the FT with respect to both momentum and frequency

$$\chi_{\text{SH}}^R(t, \mathbf{r}) = \frac{2}{\pi} \int_{2\Delta}^{+\infty} d\omega \sin(\omega t) \text{Im } \chi_{\text{SH}}^R(\omega, \mathbf{r}) = -\frac{1}{\pi} \text{Re} \int_{2\Delta}^{+\infty} d\omega (e^{i\omega t} - e^{-i\omega t}) \chi_{\text{SH}}^R(\omega, \mathbf{r}). \quad (\text{S40})$$

Let us first consider the 3D case first. To this end, we can use our result in Eq. (S38). We first introduce a dimensionless integration variable z as $\omega = 2\Delta + z/t$. Then we assume (and verify later) that $\Delta t \gg 1$ is much greater than the typical values of $|z|$ that are important for the integral. Under this assumption, the logarithm of $\omega/2\Delta - 1$ in the expression for ξ_ω can be replaced with the logarithm of Δt . This allows us to write

$$\chi_{\text{SH}}^R(t, \mathbf{r}) \approx -\frac{1}{\pi^2 \xi^2 r t \ln(\Delta t)} \text{Re} \left(e^{-2i\Delta t} \left[I((1+i)\varkappa^{1/4}) - I((1-i)\varkappa^{1/4}) \right] \right). \quad (\text{S41})$$

Here we introduced a dimensionless parameter \varkappa and a function of a complex variable $I(x)$, defined as

$$\varkappa = \frac{\pi^2 (r/\xi)^4}{\Delta t \ln^2(\Delta t)}, \quad I(x) = \int_0^{+\infty} dz \exp \left\{ -iz - xz^{1/4} \right\}. \quad (\text{S42})$$

We will evaluate $I((1 \pm i)\varkappa^{1/4})$ by the stationary phase method assuming $\varkappa \gg 1$. For $x = (1-i)\varkappa^{1/4}$, the saddle point is given by $z_* = \frac{\varkappa^{1/3}}{4} e^{i\frac{\pi}{3}}$. The function in the exponential evaluated at z_* is $-\frac{3}{4} e^{-i\pi/6} \varkappa^{1/3}$. The remaining Gaussian integral yields

$$I((1-i)\varkappa^{1/4}) \approx \sqrt{\frac{2\pi}{3}} \varkappa^{1/6} \exp \left\{ -\frac{3}{4} e^{-i\pi/6} \varkappa^{1/3} - \frac{i\pi}{12} \right\}. \quad (\text{S43})$$

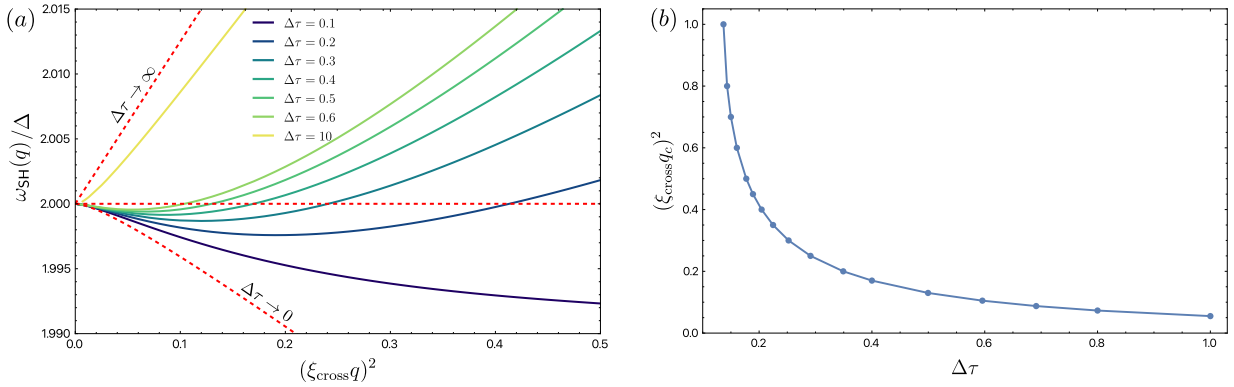


FIG. S2. (a) Dispersion of the SH mode for different values of $\Delta\tau$ in 2D, as a function of $(\xi_{\text{cross}}q)^2$. Here $\xi_{\text{cross}} = \xi_{\text{clean}}/\sqrt{1 + 2\xi_{\text{clean}}/(v_F\tau)}$ is the coherence length interpolating between $\xi = \sqrt{D/\Delta}$ and $\xi_{\text{clean}} = v_F/\Delta$ (note that ξ_{cross} depends on $\Delta\tau$, so the same value of $\xi_{\text{clean}}q$ for different $\Delta\tau$ corresponds to different momenta q). The top (bottom) red dashed line is the asymptotic clean (dirty) limit. (b) The critical value of momentum such that $\omega_{\text{SH}}(q_c) = 2\Delta$.

It turns out that the saddle point in $I((1+i)\varkappa^{1/4})$ is located on the negative real axis, on top of the branch cut of $z^{1/4}$. Thus, it is inaccessible, and the contribution of $I((1+i)\varkappa^{1/4})$ can be ignored. The result then reads as

$$\text{Re} \left(e^{-2i\Delta t} \left[I((1+i)\varkappa^{1/4}) - I((1-i)\varkappa^{1/4}) \right] \right) \approx -\sqrt{\frac{2\pi}{3}} \varkappa^{1/6} e^{-\frac{3\sqrt{3}}{8}\varkappa^{1/3}} \cos \left(\frac{3}{8}\varkappa^{1/3} - 2\Delta t - \frac{\pi}{12} \right). \quad (\text{S44})$$

We demonstrate the accuracy of this approximation in Fig. S1(c). We also note that the typical $|z|$ involved in this saddle point estimation is of the order of $\varkappa^{1/3}$. Therefore, for our initial assumption to be self-consistent, we need to have $\Delta\tau \gg \varkappa^{1/3}$, i.e. $\Delta t \ln^{1/2} \Delta t \gg r/\xi$. Given the $z = 4$ dynamical scaling, the oscillations of interest occur at $r/\xi \sim (\Delta\tau)^{1/4} \ln^{1/2} \Delta\tau \ll \Delta\tau$, so our result is well within the regime of control.

After combining these expressions, we find

$$\chi_{\text{SH}}^R(t, \mathbf{r}) \approx \frac{\Delta}{\sqrt{3/2}\pi^{7/6}\xi^3} \times \frac{e^{-\frac{3\sqrt{3}}{8}\varkappa^{1/3}}}{(r/\xi)^{1/3}(\Delta t)^{7/6} \ln^{4/3}(\Delta t)} \cos \left(\frac{3}{8}\varkappa^{1/3} - 2\Delta t - \frac{\pi}{12} \right), \quad d = 3. \quad (\text{S45})$$

In the 2D case, the integral in Eq. (S42) contains an extra factor $1/z^{1/8}$ which should be evaluated at the saddle point z_* . The result is given in Eq. (13) of the main text.

CROSSOVER BETWEEN THE DIRTY AND CLEAN REGIMES FOR THE SH POLE

According to our analysis in the preceding sections, in addition to the late-time oscillations in $\chi^R(t, \mathbf{q})$ with frequency 2Δ , there is another contribution with a q -dependent frequency $\omega_{\text{SH}}(\mathbf{q})$ that appears only when the SH pole is “visible,” i.e., when $\omega_{\text{SH}}(\mathbf{q}) > 2\Delta$ (cf. Eq. (S33) and Eq. (10) of the main text). In the dirty limit ($\Delta\tau \ll 1$), we find that $\omega_{\text{SH}}(\mathbf{q}) < 2\Delta$. However, in the clean (ballistic) regime ($\Delta\tau \gg 1$) this frequency behaves as $\omega_{\text{SH}}(\mathbf{q}) - 2\Delta \propto \xi_{\text{clean}}^2 q^2$, where $\xi_{\text{clean}} = v_F/\Delta$ is the coherence length in the absence of disorder. In this section, we numerically analyze the transition between these two limits. To this end, we first define a crossover coherence length as $\xi_{\text{cross}} = \xi_{\text{clean}}/\sqrt{1 + 2\xi_{\text{clean}}/(v_F\tau)}$, which tends to ξ_{clean} as $\Delta\tau \rightarrow \infty$ and approaches $\xi = \sqrt{D/\Delta}$ in the dirty limit ($\Delta\tau \ll 1$). Hence, it is natural to measure momentum in units of ξ_{cross}^{-1} . Next, we employ the full expression for the imaginary part of $1/\chi_{\text{SH}}^R(\omega, \mathbf{q})$ (Eq. (S22), which is valid for arbitrary $\Delta\tau$) together with the modified Kramers–Kronig relation (Eq. (S24)) to obtain $\chi_{\text{SH}}(z, \mathbf{q})$, and then construct $\chi_{\text{SH}}^\downarrow(z, \mathbf{q})$ using Eq. (A1) in End Matter. The analytic continuation of the spectral density, $\rho_{\mathbf{q}}(\omega) \equiv \text{Im} 1/\chi_{\text{SH}}^R(\omega \geq 2\Delta, \mathbf{q})$, to the lower half-plane is obtained directly from the integral representation in Eq. (S22) after the change of variable $\tilde{E} = (E - \Delta)/(|\omega| - 2\Delta)$, which maps the integration interval to $\tilde{E} \in [0, 1]$. The resulting SH dispersion relation $\omega_{\text{SH}}(\mathbf{q})$ as a function of $(\xi_{\text{cross}}q)^2$ (for $(\xi_{\text{cross}}q)^2 \leq 0.5$) is shown in Fig. S2(a) for various values of $\Delta\tau$ in 2D. As $\Delta\tau$ increases, the critical momentum $\xi_{\text{cross}}q_c$ (such that $\omega_{\text{SH}}(q_c) = 2\Delta$) decreases, and the dispersion relation approaches the clean limit $\omega_{\text{SH}}(\mathbf{q}) \approx 2\Delta + \xi_{\text{clean}}^2 q^2/8$. The dependence of $\xi_{\text{cross}}q_c$ on $\Delta\tau$ is further illustrated in Fig. S2(b).

NONLINEAR CURRENT RESPONSE

In this section, we consider a nonlinear current response due to an external oscillating vector potential $\mathbf{A}(t, \mathbf{r}) = \mathbf{A}_{\omega, q} e^{i\mathbf{q}\cdot\mathbf{r} - i\omega t}$. The total paramagnetic contribution to the electric current at the cubic order $\mathbf{A}_{\omega, q}^3$ has the form $\mathbf{J}(t, \mathbf{r}) = \mathbf{J}_{3\omega, 3q} e^{3i\mathbf{q}\cdot\mathbf{r} - 3i\omega t}$, where

$$\mathbf{J}_{3\omega, 3q} = \mathbf{J}_{3\omega, 3q}^{(\text{qp})} + \mathbf{J}_{3\omega, 3q}^{(\text{SH})}. \quad (\text{S46})$$

The SH contribution to the current can be further expressed as

$$\begin{aligned} \mathbf{J}_{3\omega, 3q}^{(\text{SH})} &= 4\pi\nu D^2 \chi_{\text{SH}}^R(2\omega, 2q) \mathcal{B}_{\text{SH}}^R(\omega, q) |\mathbf{A}_{\omega, q}|^2 \mathbf{A}_{\omega, q}, \\ \mathcal{B}_{\text{SH}}^R(\omega, q) &= -2\pi B_1^R(\omega, 2q) B_2^R(\omega, 2q). \end{aligned} \quad (\text{S47})$$

The factors $B_1^R(\omega, 2q)$ and $B_2^R(\omega, 2q)$ are the fermionic loops, each connecting two external vector potential vertices to the SH propagator. The diagrammatic calculation of these functions is a straightforward generalization of the $q = 0$ results of [9] to finite q . On the Matsubara axis and for $\Delta\tau \ll 1$, we find

$$B_1(i\omega_n, q) = \Delta T \sum_{m \geq 0} \frac{\omega_n^2 - 3\varepsilon_m^2 + \Delta^2 - E_{\varepsilon_m + |\omega_n|} E_{\varepsilon_m - |\omega_n|}}{(Dq^2 + E_{\varepsilon_m + |\omega_n|} + E_{\varepsilon_m - |\omega_n|}) E_{\varepsilon_m} E_{\varepsilon_m + |\omega_n|} E_{\varepsilon_m - |\omega_n|}}, \quad (\text{S48})$$

and

$$\begin{aligned} B_2(i\omega_n, q) &= \Delta T \sum_{m \geq 0} \frac{1}{(Dq^2 + E_{\varepsilon_m + |\omega_n|} + E_{\varepsilon_m - |\omega_n|}) E_{\varepsilon_m + |\omega_n|} E_{\varepsilon_m - |\omega_n|}} \left\{ \left(\frac{1}{E_{\varepsilon_m + 2|\omega_n|}} + \frac{1}{E_{\varepsilon_m - 2|\omega_n|}} \right) \right. \\ &\quad \left. \times (\Delta^2 + \omega_n^2 - \varepsilon_m^2 - E_{\varepsilon_m + |\omega_n|} E_{\varepsilon_m - |\omega_n|}) - 2\varepsilon_m \left(\frac{\varepsilon_m + 2|\omega_n|}{E_{\varepsilon_m + 2|\omega_n|}} + \frac{\varepsilon_m - 2|\omega_n|}{E_{\varepsilon_m - 2|\omega_n|}} \right) \right\}. \end{aligned} \quad (\text{S49})$$

In addition, the quasiparticle contribution, $\mathbf{J}_{3\omega, 3q}^{(\text{qp})}$, is given by

$$\mathbf{J}_{3\omega, 3q}^{(\text{qp})} = -4\pi\nu D^2 B_3^R(\omega, 2q) |\mathbf{A}_{\omega, q}|^2 \mathbf{A}_{\omega, q} \quad (\text{S50})$$

where $B_3^R(\omega, q)$ is obtained from analytic continuation of the following Matsubara sum

$$\begin{aligned} B_3(i\omega_n, q) &= T \sum_{m \geq 0} \frac{1}{(Dq^2 + E_{\varepsilon_m + |\omega_n|} + E_{\varepsilon_m - |\omega_n|}) E_{\varepsilon_m}} \left\{ \varepsilon_m \left(\frac{\varepsilon_m + 2|\omega_n|}{E_{\varepsilon_m + 2|\omega_n|}} + \frac{\varepsilon_m - 2|\omega_n|}{E_{\varepsilon_m - 2|\omega_n|}} \right) \times \right. \\ &\quad \left. \times \left(1 - \frac{\varepsilon_m^2 - \omega_n^2 - 3\Delta^2}{E_{\varepsilon_m + |\omega_n|} E_{\varepsilon_m - |\omega_n|}} \right) + \left(1 + \frac{3\varepsilon_m^2 - \omega_n^2 - \Delta^2}{E_{\varepsilon_m + |\omega_n|} E_{\varepsilon_m - |\omega_n|}} \right) \left(\frac{\Delta^2}{E_{\varepsilon_m + 2|\omega_n|}} + \frac{\Delta^2}{E_{\varepsilon_m - 2|\omega_n|}} \right) \right\}. \end{aligned} \quad (\text{S51})$$

After performing analytic continuation of the factors $B_{1,2,3}$ in Eqs. (S48-S51), we obtain Eqs.(C2-C6) in End Matter.

-
- [1] P. W. Anderson, Theory of dirty superconductors, *J. Phys. Chem. Solid* **11**, 26 (1959).
 - [2] A. A. Abrikosov and L. P. Gor'kov, On the theory of superconducting alloys, I. The electrodynamics of alloys at absolute zero, *Sov. Phys. JETP* **8**, 1090 (1959).
 - [3] A. A. Abrikosov and L. P. Gor'kov, Superconducting alloys at finite temperatures, *Sov. Phys. JETP* **9**, 220 (1959).
 - [4] P. A. Lee and T. V. Ramakrishnan, Disordered electronic systems, *Rev. Mod. Phys.* **57**, 287 (1985).
 - [5] A. D. Mirlin, Statistics of energy levels and eigenfunctions in disordered systems, *Physics Reports* **326**, 259 (2000).
 - [6] I. O. Kulik, O. Entin-Wohlman, and R. Orbach, Pair susceptibility and mode propagation in superconductors: A microscopic approach, *J. Low Temp. Phys.* **43**, 591 (1981).
 - [7] E. Andriyakhina, P. Nosov, S. Raghu, and I. Burmistrov, Quantum fluctuations and multifractally enhanced superconductivity in disordered thin films, *J. Low Temp. Phys.* , 1 (2024).
 - [8] D. Phan and A. V. Chubukov, Following the Higgs mode across the BCS-BEC crossover in two dimensions, *Phys. Rev. B* **107**, 134519 (2023).
 - [9] M. Silaev, Nonlinear electromagnetic response and higgs-mode excitation in bcs superconductors with impurities, *Phys. Rev. B* **99**, 224511 (2019).